Detecting Rice Cropping Patterns with Sentinel-1 Multitemporal Imagery

KUAN CHAI
February, 2018

SUPERVISORS:
Prof. Dr. Andy Nelson
Dr. Roshanak Darvishzadeh

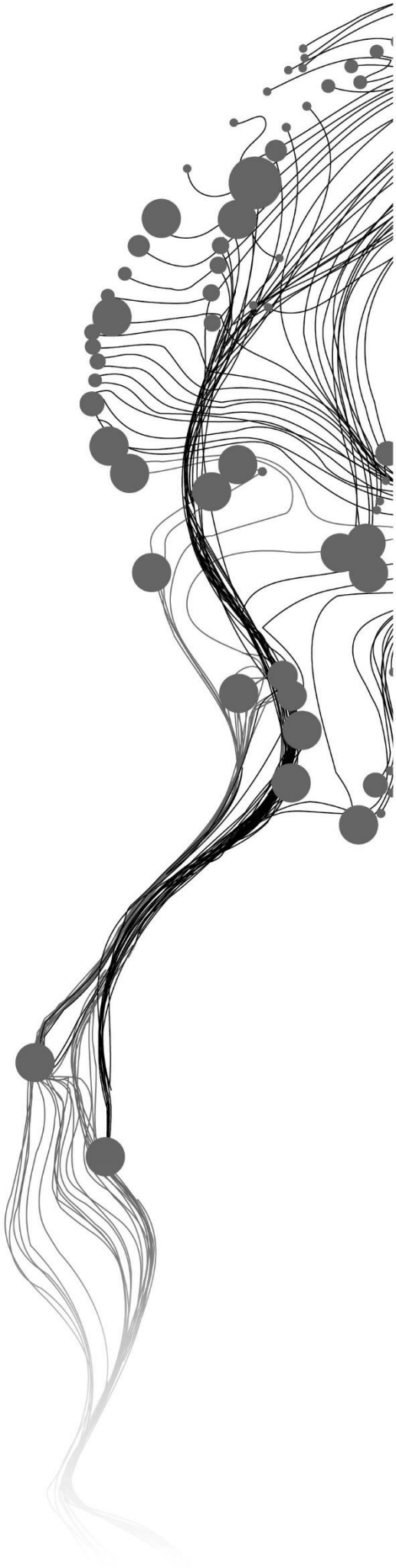

Detecting Rice Cropping Patterns with Sentinel-1 Multitemporal Imagery

KUAN CHAI
Enschede, The Netherlands, February, 2018

Thesis submitted to the Faculty of Geo-Information Science and Earth Observation of the University of Twente in partial fulfilment of the requirements for the degree of Master of Science in Geo-Information Science and Earth Observation.
Specialization: Natural Resources Management

SUPERVISORS:
Prof. Dr. Andy Nelson
Dr. Roshanak Darvishzadeh

THESIS ASSESSMENT BOARD:
Dr. C.A.J.M. de Bie (Chair)
Dr. M. Boschetti (External Examiner)

ABSTRACT

Rice-based cropping patterns, where rice is at least one crop in sequence of crops grown on the same plot of land in one year, are common throughout Asia and have significant agricultural, economic and environmental value. However, they are rarely reported in annual agricultural statistics which report rice area and production per season but not the area per cropping pattern. Multi- or hyper-temporal remote sensing data can offer a cost-effective way to detect cropping patterns on a large scale. Synthetic Aperture Radar (SAR) imagery is highly suitable for discriminating among crop types due to its sensitivity to crop canopy structure and water content. Sentinel-1 has higher spatial and temporal resolution SAR imagery compared to other microwave sensors and provides an opportunity to detect the cropping patterns in the small rice fields typical of much of rice growing in Asia.

The objective of this study is to use high-spatial-resolution Sentinel-1 multitemporal imagery to detect rice-based cropping patterns in the major rice-growing area of the Philippines, including (1) determining the best polarization or band ratio to differentiate different rice cropping patterns, and; (2) comparing the performance of rule-based and decision tree classifiers in classifying different cropping patterns. To realize the objectives, we collected 100 farmer interviews and 124 field observations during the field survey, conducting from 24th September to 9th October 2017. A total of 30 dual-polarization images across two provinces (Nueva Ecija and Tarlac) in the Philippines were obtained between November 2016 and October 2017.

In this study, we demonstrated that VH was the best single polarization to detect different cropping patterns among VV, VH and ratio of VV/VH. We also defined agronomically relevant parameters and the corresponding temporal features to discriminate between cropping patterns. A set of rules and thresholds for these temporal features, based on VH polarization, were generated using decision tree and rule-based classifiers to classify four rice-based cropping patterns (rice-rice, other-rice, rice-fallow, fallow-rice). The predictive performance of the two classifiers were compared in terms of overall accuracy and kappa coefficient using separate training and validation datasets. The highest overall accuracy (83%) was obtained for the rule-based classifier compared to the decision tree classifier (76%) from the validation results. To our knowledge, this is the first time that multitemporal Sentinel-1A imagery has been used to delineate rice cropping patterns at field level and a high accuracy was obtained using a rule-based algorithm.

ACKNOWLEDGEMENTS

I would like to express my profound gratitude to:

The following at the Faculty of Geo-Information Science and Earth Observation (ITC): The ITC Directorate for giving me the opportunity to complete the MSc through the UTS-ITC Excellence Scholarship programme. Prof. Dr. Andy Nelson and Dr. Roshanak Darvishzadeh who gave their professional supervision, patience and dedication throughout my thesis study. Dr. Kees de Bie for the advice and suggestions to improve the thesis. Vidya Nahdhiyatul Fikriyah and Sravan Shrestha for the collaboration in the field data collection and preparation. Wenfei Dong for her continued encouragement and support.

The following during the fieldwork in Central Luzon, Philippines: 100 farmers in who participated in the surveys; the barangay officials in the 15 villages who helped coordinate the survey/field visits; Neale Paguirigan and Ronald Castro for interview translation, data preparation, assistance with field measurements and logistics, and; our drivers, Dennis and Fred, for their willingness to help out and get their feet wet.

The following at the PhilRice Central Experiment Station (CES), Muñoz, Nueva Ecija, Philippines: Dr. Eduardo Jimmy P. Quilang for supporting our research and our stay at the CES; our test farmers Sonia Asilo and Rose Mabalay, for their advice to improve the survey; Jaja Bibar for arranging accommodation and meetings with PRISM/PRIME project staff at PhilRice CES; Rose Mabalay for facilitating access to water release dates for the main irrigation systems in Nueva Ecija, and; Sonia Asilo for permission to use her published rice cropping system map.

The following at the International Rice Research Institute (IRRI), Los Baños, Philippines: Dr. Alice Laborte for supporting and collaborating in this research and facilitating access to irrigation system boundary data, existing household survey and field data from CLLS, PRISM and MISTIG; Ludy Velasco for validating our survey route and for the ITC hats; Tintin Doctolero for logistics, and; IRRI Education for administrative arrangements related to our internship at IRRI.

We also thank the PRISM management team and DA-BAR Director Dr. Nicomedes Eleazar for granting us access to a subset of PRISM data.

TABLE OF CONTENTS

LIST OF FIGURES

LIST OF TABLES

ABBREVIATIONS

CE: Crop Establishment

CLLS: Central Luzon Loop Survey

DN: Digital Number

DS: Dry Season

DT: Decision Tree

FAO: Food and Agriculture Organization

GEO: Group on Earth Observation

GEOGLAM: Group on Earth Observation Global Agricultural Monitoring Initiative

GRD: Ground Range Detected

HA: Harvest

IRRI: International Rice Research Institute

IW: Interferometric Wide

LP: Land Preparation

NIA: National Irrigation Administration

NIS: National Irrigation System

PRiSM: Philippine Rice Information System

PoS: Peak of Season

SoS: Start of Season

SAR: Synthetic Aperture Radar

SNAP: Sentinel Application Platform

SRTM: Shuttle Radar Topography Mission

WS: Wet Season

1. INTRODUCTION

1.1. Background

Rice is an important crop for food security in many countries, especially in Asia where it dominates overall crop production and overall food consumption to a much greater extent than elsewhere in the world (Pandey, Byerlee, & Dawe, 2010). Stable and sustainable rice production requires information on where, when and how rice is grown (Cuerdo et al., 2013; Hijmans, 2007). Several countries have developed information systems to monitor rice production such as in the Philippines where the Philippine Rice Information System (PRiSM) has recently been implemented. Also, some global systems have been set up, for example, the GEO Global Agricultural Monitoring (GEOGLAM), to enhance global crop production projections by coordinating satellite monitoring observation systems in different regions of the world. Although these systems estimate the area and production of rice, they do not directly report on the area of rice that is planted in different cropping systems. The cropping system refers to a system, comprising soil, crop, weeds, pathogen and insect subsystems, that transforms solar energy, water, nutrients, labour and other inputs into food, feed, fuel or fibre (FAO, 1996). A subset of the cropping system comprises the cropping pattern, which refers to the yearly sequence and spatial arrangement of crops or crops and fallow in a particular land area (FAO, 1996).

Rice can be grown more than once per year in the same field and can be grown in a monoculture (two or three rice crops per year) or in a system where rice is grown in one season and another crop (such as wheat, maize or vegetables) is grown in the other season (FAO, 2005). Some areas even switch between rice and aquaculture in the same year. A key characteristic of a cropping pattern is the bare fallowing between two sequential cultivations, practised by leaving a field unplanted or unutilized for another productive purpose for a short or long duration (Aweto, 2013).

The size and distribution of rice areas in Asia between 2000-2009 across four cropping patterns (rice-fallow, rice-other, rice-rice or rice-rice-rice, rice-rice-other) have been estimated by Pandey et al. (2010) and is shown in Table 1.1.

Table 1.1 Rice area by cropping system and water source for Asian regions, 2000-2009 (Pandey et al., 2010)

Cropping system	South Asia	Southeast Asia	East Asia	Total
Irrigated	30.6	19.6	30.7	80.8
Rice-fallow	9.5	0.8	10.2	20.6
Rice-other	13.9	1.7	5.7	21.3
Rice-rice or rice-rice-rice	5.7	10.5	5.6	21.8
Rice-rice-other	1.4	6.5	9.2	17.2
Rainfed	30.7	27.3	2.3	60.3
Rice-fallow	21.1	11.0	2.3	34.4
Rice-other	4.2	5.7	0.0	9.9
Rice-rice	5.4	10.6	–	16.0
Grand total	61.3	46.9	33.0	141.2

Sources of data: compiled by IRRI from IRRI (2010), Huke and Huke (1997), Hijmans (2007), FAO (2002), Maclean et al (2002), Portmann et al (2008), Frolking et al (2002, 2006), and Gumma et al (forthcoming).

The estimates of how much rice is grown under each of these cropping patterns in rice-planted regions are at the continent level and not specific to countries; they are rarely reported in national annual agricultural

statistics which report crop area and production per season but not the area per cropping pattern over one year.

Different cropping patterns have different requirements for their implementation and management and have different impacts on the environment and the economy (Singh, Singh, & Chitale, 2014). Regarding water management, for example, more crops of rice per year tend to be grown in the irrigated system than the rainfed system, which means more intensive double or triple rice-cropping patterns dominate in water sufficient areas (Pandey et al., 2010). In terms of impacts on the economy, different rice cropping patterns have different economic value. Parihar et al. (1999) reported that cultivation cost in India was highest in rice-rice patterns while the net return was more or less the same in rice-rice, rice-wheat and rice-peanut cropping patterns.

Also, in relation to environmental benefits, different cropping patterns and the accompanying bare fallow contribute to the control and prevention of pests and diseases (Koshy, Nair, & Kumar, 2008; Umaerus, 1992). Pests and diseases are frequently the most serious problems for rice crop health and management, causing significant losses in crop yield (Winch, 2006). According to Winch (2006), the percentage of crop yield damaged by insects was estimated as follows: Europe 5%, North and Central America 9%, South America 10%, Africa 13% and Asia 21%, and that plant diseases were estimated to cause almost 10% loss in crop yield globally. Planting sequential multiple crops in the same field has many benefits including, for instance, reducing the accumulation of disease, insects and weeds, enhancing biodiversity on a landscape level as well as improving soil fertility (Steinmann & Dobers, 2013; Winch, 2006). Fallow practice between two cultivations is also considered as a cheap and efficient strategy for soil nutrient restoration and weeds prevention (Ikuenobe & Anoliefo, 2003; Randriamalala et al., 2012; Nielsen & Calderon, 2011). Available soil nitrogen increases and weeds are controlled during the fallow period (Stewart, 1999). Furthermore, short or long fallow periods differ in plant diversity, density, and composition in shifting cultivation fields (Dalle & Blois, 2006). Moreover, tree and shrub regeneration are reduced by longer cropping periods, more frequent weeding, greater crop cover, and shorter fallow periods (Staver, 1991). Thus, a better understanding of where and when these cropping patterns occur can help policy makers to decide on what type of implementation or management is needed to improve crop yield and what interventions could improve the suitability or sustainability of those cropping patterns.

In short, better information on cropping patterns can give a better perspective on rice crop health and management, minimising damage to rice crop and reducing the production loss. This kind of information has significant agricultural, economic, and environmental value (Singh et al., 2014).

1.2. Literature review

Considering the extent and significance of rice cropping patterns, it is necessary for farming systems researchers as well as agriculture planners and land managers to collect and monitor spatial information of cropping patterns (Liew et al., 1998). The traditional way, which involves high cost and labour, is to gather such information over large areas by the ground survey (Mansaray et al., 2017). However, this method is not applicable to current demands which require rapid and timely updates on the distribution and area per rice cropping pattern.

Fortunately, multi- or hyper-temporal remote sensing techniques can offer a cost-effective way to detect cropping patterns on a large-scale landscape, due to the sensitivity of remote sensors to crop texture variations and their capability to capture the temporal signature of crops (Asilo et al., 2014).

Figure 1.1 shows the growth of rice plants, cultivated in tropical or subtropical conditions, which is commonly divided into three main crop phases: vegetative, reproductive and ripening (Vergara, 1992).

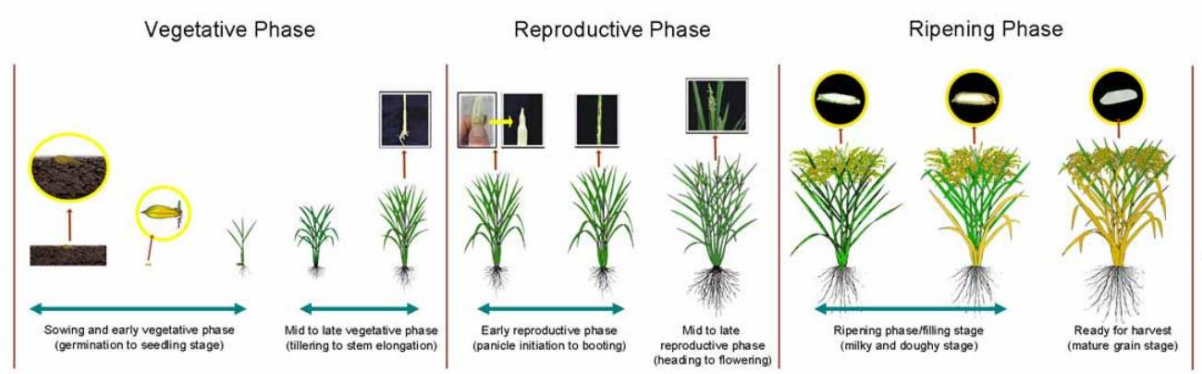

Figure 1.1 Rice growth phases
(source: http://www.knowledgebank.irri.org/step-by-step-production/pre-planting/crop-calendar**)**

The first phase is the vegetative phase (from 45 to 100 days) which consists of the germination, seedling, tillering and stem elongation stages. Germination starts when the seeds are sown in the wet soil and it results in the formation of the seedling. Tillering starts about 15 days after sowing and continues until flowering (Le Toan et al., 1997). At the later stage of tillering, towards the panicle initiation stage, stem elongation begins and contributes to a rapid increase in the vertical expansion of the rice canopy (Nelson et al., 2014). It is followed by the reproductive phase (around 35 days) which includes the panicle initiation, heading, and flowering stages. During this phase, the plant is characterized by a decrease of the number of tillers, the development of paniculate leaf, panicle formation, and grain development (Le Toan et al., 1997). Ripening is the final phase (around 30 days) with its milk, dough and mature grain stages (De Datta, 1981). Irrigation is stopped in the field from ripening up to harvest and the overall plant water content decreases (Le Toan et al., 1997; Nelson et al., 2014).

Rice fields are usually inundated during the planting and vegetative stage, and detection of this is a key element of most remote-sensing rice detection algorithms (Boschetti et al., 2014). However, for other crops, wheat, for example, is not flooded by irrigated water during the vegetative phase, but the growth duration and phases can be similar to rice (see Figure 1.2). As for fallow land that remains unplanted between two cultivations, there is usually little or no vegetation.

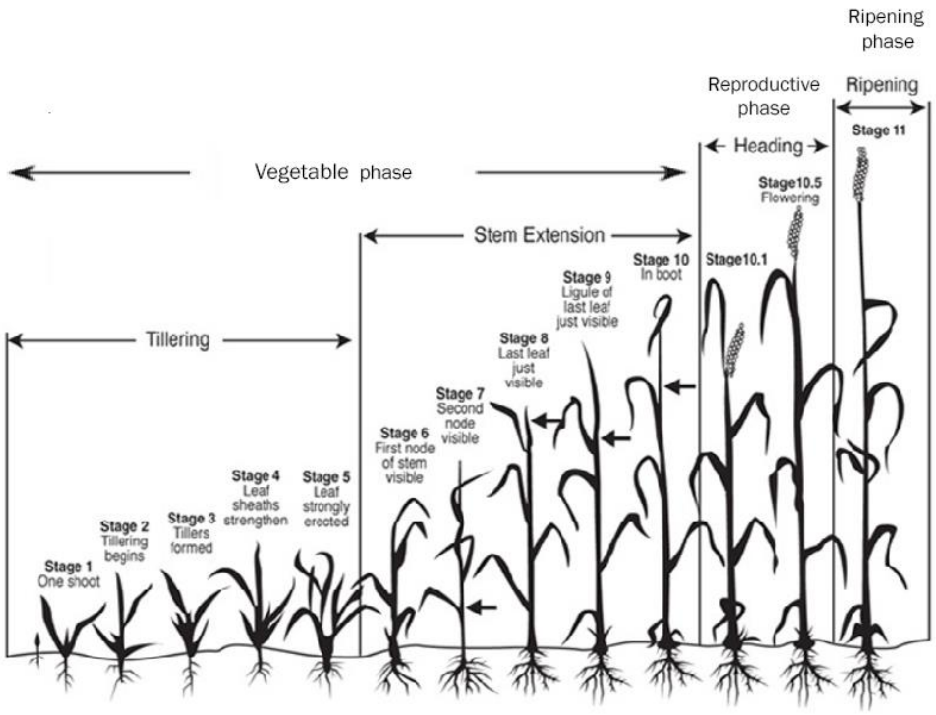

Figure 1.2 Wheat growth stages
(source: http://prairiecalifornian.com/wheat-growth-stages**)**

These crop phases coincide with spatial and temporal changes in plant growth. Changes in plant growth can be detected due to changes in the interaction of the plant with light and microwaves and thus can be observed by remote sensing data (Nguyen et al., 2015). That means that each crop (such as rice, wheat, maize, bean, vegetable) has distinct growth phases and that the changes in the crop biomass, canopy, water content over time can be used to distinguish different crops. Given the diversity of cropping patterns, it is difficult to discriminate the different cropping patterns using one single-date image (Liew et al., 1998). Detecting rice cropping patterns requires analysis of dense time series to distinguish rice from other crops or fallow (Nguyen et al., 2015), as such, a rice-rice pattern would be different from rice-fallow because of the distinct temporal pattern.

Passive remote sensing data from optical sensors have been utilized to delineate rice cropping systems and crop patterns using time series images. Regarding the application of optical sensors to map rice-based cropping systems, most studies were conducted in countries or regions with very large rice growing areas. For example, Gumma et al. (2014) mapped rice cropping intensity in Bangladesh using MODIS 8-day composite data with 500 m spatial resolution. Manjunath et al. (2006) derived the rice rotation map In India using IRS WiFS data with 188 m spatial resolution and 5-day revisit capability, Nguyen et al. (2012) mapped the Mekong Delta rice cropping patterns using 10-day SPOT VGT NDVI 1 km spatial resolution imagery. Also in the Philippines, Asilo et al. (2014) used 8-day composite MODIS NDVI data to map rice cropping patterns in Nueva Ecija and Pangasinan provinces. Similar works have also been done using Landsat TM (Martínez-Casasnovas et al., 2005) and IRS-1A & IRS-1B images (Panigrahy & Sharma, 1997). Although high temporal data is available using optical sensors, most of these studies focused on large landscapes and due to the relatively low spatial resolution they were not able to detect small rice fields.

Active remote sensors, that can penetrate cloud cover, such as Synthetic Aperture Radars (SAR) can capture the temporal backscatter signature of different crops. Backscatter is the portion of the outgoing radar signal that the crop reflects directly back towards the radar antenna. It is a function of radar system

characteristics, topography, and properties of the crops. Crop canopy structure and water content vary as a function of crop type, growth stage and crop condition, and these variations can be detected by SAR sensors to differentiate among crop types (McNairn et al., 2009). A key to successful crop classification is to understand which growth stages are best for crop separation (McNairn & Shang, 2016). McNairn et al. (2009) found that using SAR images acquired late in the growing season provided best overall accuracy for classifying canola, soybean, and wheat. Deschamps et al. (2012) recommended using a SAR image acquired during the seed and reproductive phenology stages, at the point of peak biomass, to achieve better discrimination among crop types.

Most paddy fields experience agricultural inundation before crop establishment, which is different from lands covered with other crops, such as maize, beans, and vegetables. Low backscatter during the transplanting stage and a high backscatter during the early growing stages result in large and rapid changes in the temporal SAR backscatter profile, and this feature can be utilized for discriminating rice from other crops (Oyoshi et al., 2016). For delineation and classification of rice-cropping systems, Liew et al. (1998) derived temporal backscatter profiles from 35-day ERS-2 imagery to classify crop rotations. Bouvet et al. (2009) and Nguyen et al.(2015) employed a multitemporal method to map rice-cropping systems in the Mekong Delta using Envisat ASAR with 35-day revisit capability and combined 16-day revisit respectively. However, as with many optical data applications, the wide swath mode data used from ERS and ENVISAT have moderately low spatial resolution relative to the size and spatial patterns of the non-rice vegetation and other land covers (Nguyen et al., 2015), which leads to an overestimation of rice fields.

Sentinel-1 presents significant superiority over previous European SAR missions as stated above, in terms of spatial and temporal resolution, geographical coverage, reliability and data dissemination (Mansaray et al., 2017). Sentinel-1 is composed of a constellation of two satellites, Sentinel-1A and Sentinel-1B, sharing the same orbital plane (ESA, 2013). The Sentinel-1A satellite, launched on 3 April 2014, gives the opportunity to map small rice fields due to the high spatial resolution of 20 m and temporal resolution of 12 days. Furthermore, the launch of Sentinel-1B has the potential to double the revisit time for continuous radar mapping of the earth providing improved spatiotemporal coverage of the earth surface (Nguyen, Gruber, & Wagner, 2016). This satellite constellation can provide services and applications over land typically including crop monitoring, land cover mapping and change monitoring (Potin et al., 2012), therefore it can be utilized to map different cropping patterns.

The C-band Sentinel-1 SAR is a dual polarization radar, which can transmit and receive a signal in both horizontal (H) and vertical (V) polarizations (ESA, 2013). Free data products are available in single polarization (VV or HH) and dual polarization (VV+VH or HH+HV). Different polarizations have different interactions with crops due to multiple scattering events created by structure (stems, leaves, fruit) within the crop volume (McNairn & Shang, 2016). Generally, two common methods of SAR-based rice mapping have been implemented using different polarizations: (1) single polarization of backscatter data with high temporal density and (2) backscatter response from multi-polarizations (Nguyen et al., 2015). For the first method, Le Toan et al. (1997) used ERS-1 VV polarization to capture phenology of rice growth, and Shao et al. (2001) used RADARSAT HH polarization for rice monitoring and production estimation. The second method has been applied by Guo et al. (2014) who used contrast analysis of the different imagery of VH and VV to select imagery with better identification. Also, Bouvet et al. (2009) demonstrated that the ratio between HH and VV polarization on multitemporal datasets had higher accuracy and required less temporal coverage compared to a single polarization. For Sentinel-1, Nguyen et al. (2016) and Mansaray et al. (2017) showed that VH backscatter was more sensitive to rice growth than VV polarized backscatter and was thus selected to map rice areas. Furthermore, based on a literature review, no work has been done using Sentinel-1 polarizations such as the use of single polarization, combinations of VV and VH or the ratio between VV and VH to map cropping patterns, thus multiple

polarizations comparison should be implemented to select the best option before classifying different cropping patterns.

Various classification methods have been proposed for remote sensing time series data, including machine learning algorithms such as support vector machines (SVM) (Zheng et al., 2015), k-nearest neighbours (kNN) (Myint et al., 2011), random forests (RF) (Gislason, Benediktsson, & Sveinsson, 2006), artificial neural networks (ANN) (Benediktsson, Swain, & Ersoy, 1990), and decision trees (DT) (Waheed et al., 2006), have been applied to a wide range of land-use and agricultural crop classification problems (Gilbertson et al., 2017; Kucuk et al., 2016). For example, decision tree is a non-parametric classifier that takes advantages of handling discrete data, fast processing speed and interpretable classification rules (Salehi, Daneshfar, & Davidson, 2017). It uses a multistage or sequential approach to assign a class to a pixel (Pal & Mather, 2003). The supervised classification algorithms require training samples to perform the classification. However, there is a risk of over-fitting the classification and they rely on a substantial set of good-quality training data (Nelson et al., 2014). Another challenge of using these supervised classifiers for long-term classification of rice cropping patterns is selecting appropriate training datasets for different land-cover classes, due to changes in the land cover over time (Son et al., 2013). To solve these issues, an approach named knowledge-based decision rule has been introduced and successfully applied for classifying cropping systems with SAR time series. The rules of the classifier are set by the operator or user relying on expert local knowledge or other sources of information to further determine the parameter values (Nelson et al., 2014). Nguyen et al. (2015) adopted a crop phenology-based classifier to detect and map single-, double- and triple-cropped rice areas with multi-year Envisat ASAR data and also applied it to map rice fields using Sentinel-1A time series (Nguyen et al., 2016). Nelson et al. (2014) presented a simple, robust, rule-based classification for mapping rice area with multitemporal SAR imagery. The approach is based on a small number of rules and parameters that can be quickly fine-tuned from site to site and season to season (Nelson et al., 2014) using a relatively small number of training and validation observations. However, a major shortcoming of such rule-based classifier lacks automation, since the same rules and thresholds may not apply everywhere, preventing the general applicability and transferability of the approach to different images, areas, and applications (Salehi et al., 2017; Salehi, Zhang, & Zhong, 2013). This can be partially overcome if the rules are related to meaningful crop growth parameters or well-known crop characteristics at different growth stages.

In this study, we plan to compare the performance of a decision tree with an adapted rule-based classifier, which is similar with the classification model proposed by Nelson et al. (2014) and investigate the different polarizations and band ratio information from Sentinel-1 data to delineate where and what rice cropping patterns are practised in a major rice growing area of the Philippines.

1.3. Research problem statement

As agriculture becomes more intensive and modernized as a consequence of economic growth in developing countries, the agricultural ecosystem and food production will become increasingly threatened (Sakamoto, 2009). Careful assessment of the changing world of agricultural practices and cropping pattern is an essential first step to understand current and future food security issues, as well as providing insight to monitor crop health and management.

Rice cultivation in the Philippines is chosen as the subject of this study. The Philippines is the 9th largest rice producer in the world, accounting for 2.8% of global rice production. It was also the world's largest rice importer in 2010. Rice production needs to increase by 98% to meet the predicted national rice requirements in 2050 (Laborte et al., 2012). Increasing yield potential and yield stability, closing yield and

efficiency gaps, as well as reducing production losses are the essential issues (Pandey et al., 2010). Different types of irrigation systems and cultivation practices have been established under the authority of the Department of Agriculture in the Philippines (Arnaoudov et al., 2015). Cropping pattern is highly important since it affects rice production, farmers' income, and the environment (Pandey et al., 2010).

This study aims to understand where and what cropping patterns exist in a major rice-growing area of the Philippines using remote sensing technology. In the Philippines, farmers usually cultivate crops in two seasons per year. The majority of rice varieties in the country have a duration of 110-120 days (Asilo et al., 2014). Table 1.2 shows essential indicators such as number of crops (Jonsson & Eklundh, 2002; Nguyen et al., 2015), growth duration of each crop (Jonsson & Eklundh, 2002; Nguyen & Wagner, 2017; Nguyen et al., 2015), and number of fallows, that could be extracted from temporal remote sensing data for different cropping patterns.

Table 1.2 Essential indicators for different cropping pattern based on literature survey (Jonsson & Eklundh, 2002; Nguyen et al., 2015; Nguyen & Wagner, 2017)

Cropping pattern	Number of crops	Growth duration crop1 (days)	Growth duration crop2 (days)	Number of fallows
Rice-rice	2	110~120	110~120	2
Rice-nonrice	2	110~120	N/A	2
Rice-fallow	1	110~120	0	1
Fallow-rice	1	0	110~120	1
Nonrice-rice	2	N/A	110~120	2

Review of the literature shows that although Sentinel-1 has been utilized to delineate rice cultivation extent, no work has been done using multitemporal Sentinel-1 imagery to estimate where and what cropping patterns have been established in rice-planted areas. Sentinel-1 has the advantages of higher spatial and temporal resolutions compared to other microwave sensors and provides an opportunity to detect small rice fields on a province level. Sentinel-1 also provides a dual polarization capability which can be exploited for detecting cropping patterns.

The objective of this study is to use high-spatial-resolution Sentinel-1 multitemporal imagery to identify rice cropping patterns. Backscatter coefficients will be extracted from the time series images acquired once every 12 days to delineate what and where different rice cropping patterns are practised in the Philippines with a spatial resolution of 20m. Different polarizations and the band ratio will be tested to find the most discriminatory information. A decision tree and a rule-based classifier will be compared to classify the rice cropping patterns.

1.4. Research objective

1.4.1. General objective:

To detect rice-based cropping patterns using time series Sentinel-1 imagery and ground survey data.

1.4.2. Specific objective:

In order to achieve the general objective, the following specific objectives are set for the research:

- To explore the differences in temporal signatures of rice-based cropping patterns using Sentinel-1 multitemporal imagery.

- To compare the performance of a decision tree (DT) classifier with a rule-based classifier for classifying different rice-based cropping patterns.

1.5. Research question and hypothesis

For Objective 1:

- RQ1: Which polarization or band ratio can be used to find the most discriminatory temporal signatures for different cropping patterns?

Hypothesis: VH backscatter indicates the superiority over other polarizations and the band ratio in discriminating temporal signatures for different cropping patterns.

For Objective 2:

- RQ2: Which classifier can give the highest accuracy for classifying different rice cropping patterns?

Hypothesis: Rule-based classifier outperforms DT for classifying different rice cropping patterns.

1.6. Conceptual diagram

Figure 1.3 shows the conceptual diagram of this study. The boundary of the system is the provinces of Nueva Ecija and Tarlac, Philippine. Elements of the main system consist of rice fields cultivated in arable land, villages located in the study area and irrigation systems utilized by farmers. The sub-system of rice fields is characterized by different cropping patterns, which are identified by different spatial distributions and temporal growth patterns, whether rainfed or irrigated. Each cropping pattern has different phenological characteristics, fallow durations, and productivity. The farmers living in the villages plant and harvest crops twice within crop calendar per year, most use the irrigation system to control the water level. All these elements interact with each other, comprising the ecosystem in the study area. Outside the system, rainfall in the wet season supports rice crop growing in non-irrigated areas; farmers can export surplus rice production to the market. Earth observation and geo-information help identify the spatial and temporal pattern of rice cropping patterns, afterward validated by field observations and interviews.

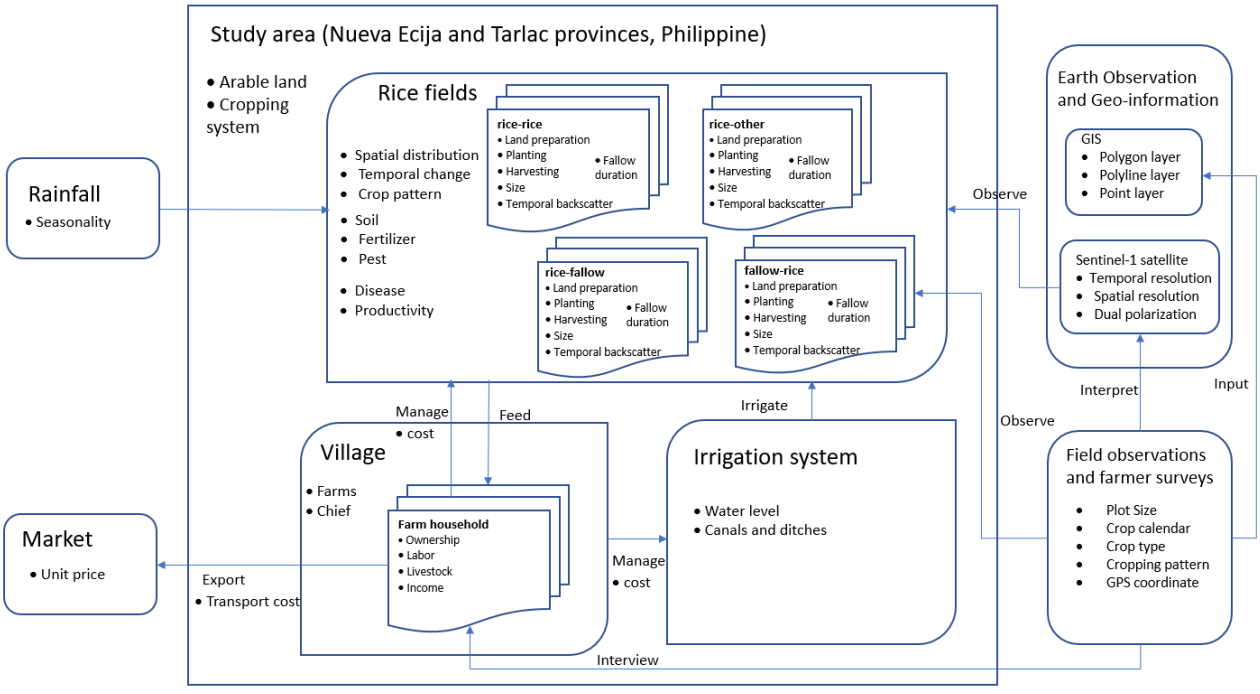

Figure 1.3 Conceptual Diagram

2. STUDY AREA AND DATA

2.1. Study area

The study area (see Figure 2.1) covers the provinces of Nueva Ecija and Tarlac located in Central Luzon, Philippines. These two provinces are the main rice producing areas in the Philippines that cover 5,751 and 3,054 km^2, respectively. In 2002, Nueva Ecija had he largest cropland area in Central Luzon, while Tarlac ranked the second (Philippine Statistics Authority, 2004). Total rice area harvested in these 2 provinces is 447,228 hectares, which comprises 66% of the total rice area in Central Luzon and 10% of total rice area of the Philippines (Philippine Statistics Authority, 2016). Other crops such as onion, peanut and maize are also cultivated by farmers but on a much smaller area.

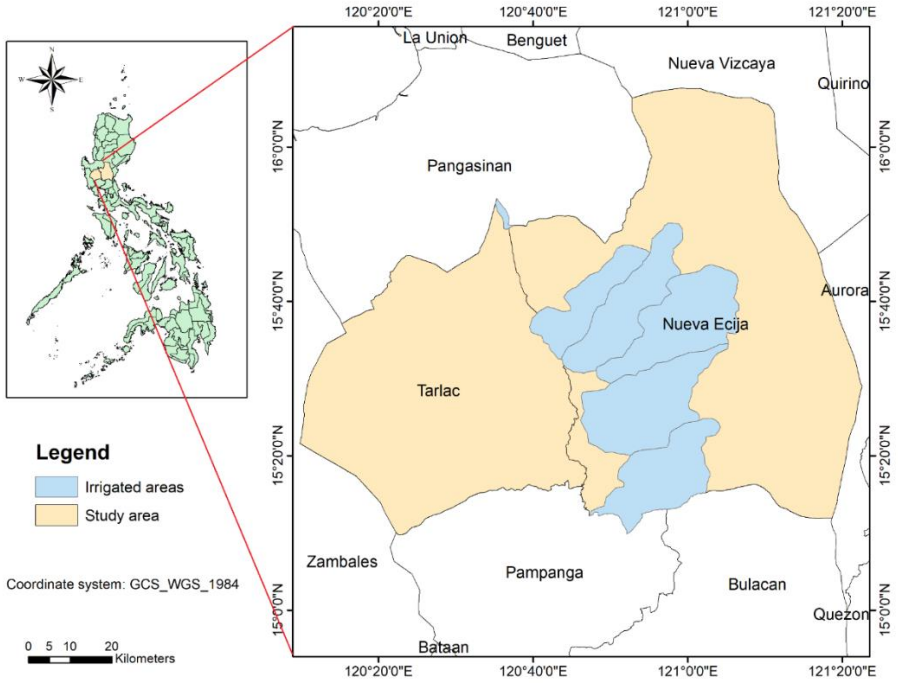

Figure 2.1 Location of study area (Nueva Ecija and Tarlac).
The inset shows the irrigated area within the study region

Nueva Ecija is characterized by a terrain that comprises mostly low alluvial plains in the west and in the southwest, and rolling uplands in the northeast (Asilo et al., 2014); In Tarlac, approximately 75% of the province is plains in the east while the rest is hilly to mountainous in the west (see Figure 2.2).

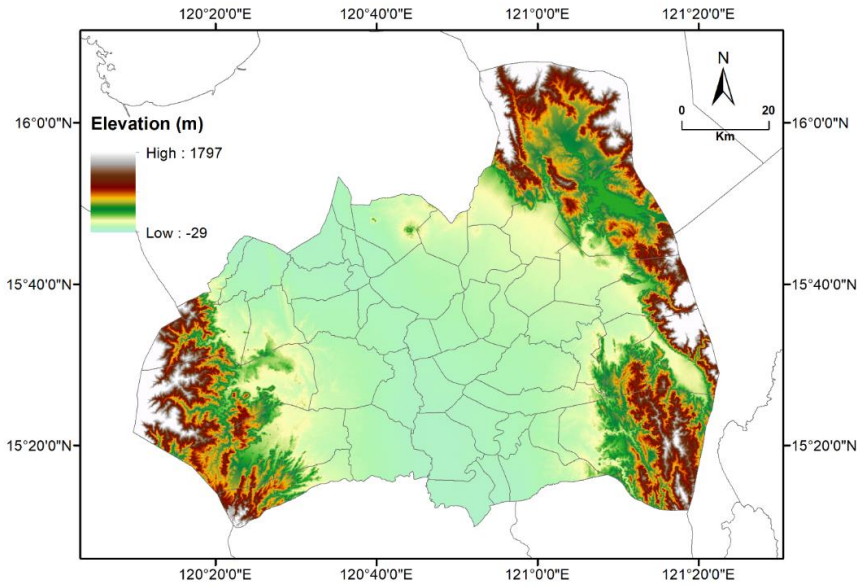

Figure 2.2 Topography of the study area

The study area has three distinct seasons: summer from March to June, monsoon rain from July to September, and monsoon winter from October to February. Figure 2.3 shows that maximum rainfall is expected to occur from July to August and is at a minimum in January or February. With irrigation, two sequential crops can be cultivated per year in this region, the first crop is sown in June, planted in late June or in July and harvested in late September or in October. The second crop is sown or planted between late December and early January and harvested in April.

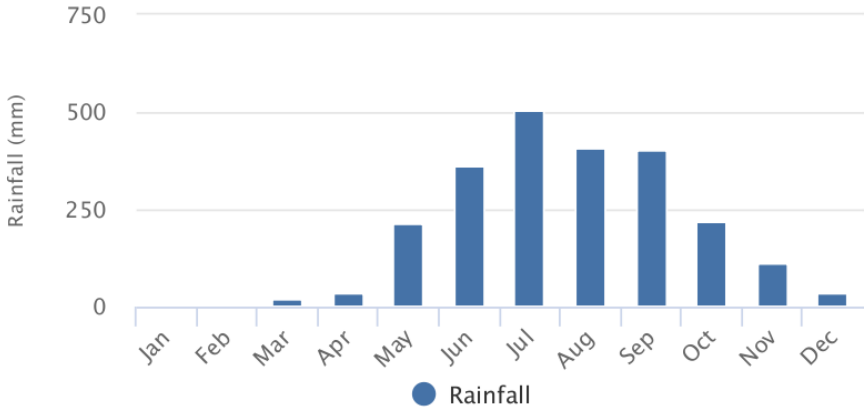

Figure 2.3 Average monthly rainfall from 1901-2015 in the study area
Source: (Climatic Research Unit of University of East Anglia, 2015)

In terms of cropping patterns, most of the study area is dominated by two seasons per year: wet season (WS) and dry season (DS). Irrigated rice is cultivated in large to medium-sized areas (blue areas in Figure 2.1) where a national irrigation system (NIS), supported by the National Irrigation Administration (NIA), exists (Asilo et al., 2014). In general, rice-rice is the dominant cropping pattern, cultivated annually in these irrigated areas. Rice-fallow and rice-nonrice cropping patterns are practised where only one rice crop is cultivated during the WS and following fallow or a non-rice crop during the DS (Asilo et al., 2014). Likewise, fallow-rice and nonrice-rice are practised by leaving land unplanted or planting non-rice crop during the WS and planting rice crop during the DS, but these only occur in areas where there is long-term flooding in the WS. These five patterns are the main rice cropping patterns in the study area. An overview of the cropping patterns per province in area is shown in Table2.1 based on Central Luzon Loop Survey data from IRRI (2015-16) (see section 2.3).

Table 2.1 The area of cropping patterns derived from CLLS in Nueva Ecija, Tarlac 2015-2016

	Area (ha)	% Share in area								
		Rice cultivation						Non-rice cultivation		
		WS DS	Rice Rice	Rice Fallow	Rice Nonrice	Fallow Rice	Nonrice Rice	Nonrice Nonrice	Nonrice Fallow	Fallow Nonrice
Nueva Ecija	870		76	17	4	1	0	1	0	1
Tarlac	395		51	15	6	24	1	3	0	1
All	1265		68	16	5	8	1	1	0	1

2.2. Sentinel-1 data

SAR multitemporal images from Sentinel-1A are used to detect and map different rice-based cropping patterns. The Sentinel-1A mission can provide C-band SAR data with 12-day revisit time including dual polarization capability (VV+VH, HH+HV), four exclusive imaging modes, different resolution (down to 5 m) and coverage (up to 400km).

For this study, free access to almost all archived Interferometric Wide Swath mode (IW) acquisitions from November 2016 to October 2017 that completely covered the study area was provided. A total of 30 images with dual polarization (VV+VH) at 20 m spatial resolution were available, which covered the seasonal rice crop calendar (rice-rice) and growth stages over one year (see Figure 2.4). The product type is Level-1 Ground Range Detected (GRD). GRD products consist of focused SAR data that has been detected, multi-looked and projected to the ground range using an Earth ellipsoid model such as WGS84. A calibration vector is included in the product allowing simple conversion of image intensity values into sigma nought values (ESA, 2013). The sigma nought (σ°), also called backscatter coefficient, is the normalized measure of the strength of radar signals reflected by a distributed target. The specifications of the Sentinel-1A time series are shown in Table 2.2.

Table 2.2 The specifications of the Sentinel-1A time series data

Satellite	Sentinel-1A
Sensor	SAR-C
Product-level	Ground Range Detected (GRD)
Order by	Descending
Date acquisition	2017.10.27 10.15 10.3 9.21 9.9 8.16 8.4 7.23 7.11 6.29 6.5 5.24 5.12 4.30 4.18 4.6 3.25 3.13 3.1 2.17 2.5 1.24 1.12 2016.12.31 12.19 12.7 11.25 11.13 11.1
Frequency (GHz)	5.045
Repeat time (day)	12
Spatial resolution (m)	20
Image Mode	Interferometric Wide swath (IW)
Polarization	VV + VH
Incidence angle (degree)	30 – 46

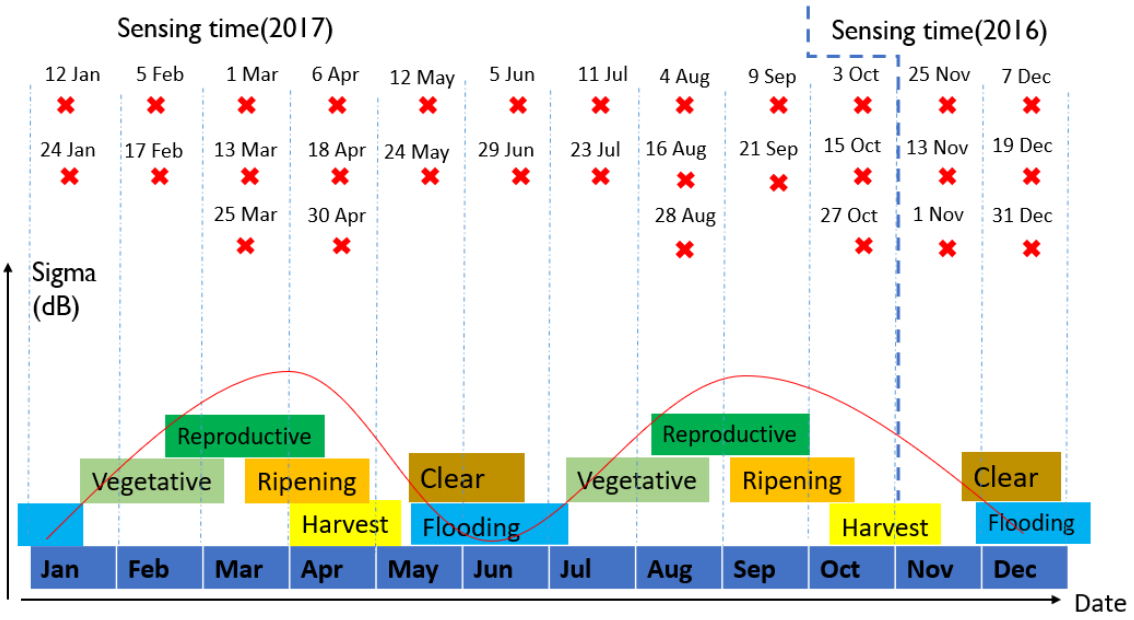

Figure 2.4 Sentinel-1 acquisition covers the seasonal rice crop calendar and growth stages (rice-rice)
Each red cross represents a Sentinel-1A acquisition date.

2.3. Existing survey data

2.3.1. Central Luzon Loop Survey (2015-16)

This survey (CLLS) was initiated by the International Rice Research Institute (IRRI) in 1966 to cover detailed records on the rice-farming practices and rice farm households in Central Luzon of the Philippines (Moya et al., 2015). The survey fields were observed in both wet and dry season at specific kilometre away from the loop of the national highway and approximately 100 sample farmers were interviewed for each survey. It is conducted every four to five years up to and including 2015-16 and 25 rounds of survey have already implemented since 1966. The survey data included GPS locations of farms, rice productivity, fertilizer, labour inputs and farm characteristics (water management, cropping pattern and crop establishment method).

The last survey was conducted by IRRI during the wet season (May -October) of 2015 and dry season (November – April) of 2016. In this study, this survey data was used to select field work locations and characterize the cropping patterns of the study area.

2.3.2. MISTIG Survey (2013-14)

The MISTIG survey was carried out by IRRI in 2013-2014 as part of a management information system (MIS) for rice research evaluation and impact assessment in Central Luzon of the Philippines. There were three stages of sampling design to select the municipalities, the villages, and the farm households. The survey randomly selected 15 municipalities in 4 provinces (Bulacan, Nueva Ecija, Pampanga, and Tarlac) that have at least 2,000 hectares of total rice area. Then four villages were randomly selected for each municipality. Finally, a systematic sampling was used to select households in each village. The survey data included GPS locations of farm households and farming practices (water management, cropping pattern and crop establishment method). The dataset was used in this study to select the farmers for interviews and subsequent observations of their farm fields.

2.3.3. 30m SRTM DEM

The Shuttle Radar Topography Mission (SRTM) datasets are active remote sensing data, obtained during an eleven-day long shuttle flight of NASA Space Shuttle Endeavour. The shuttle orbited Earth 16 times each day during the 11-day mission, completing 176 orbits. SRTM successfully collected radar data over 80% of the Earth's land surface between 60° north and 56° south latitude with data points posted every 1 arc-second (30m).

The digital elevation model (DEM) generated by SRTM data can be downloaded freely for global users (http://dwtkns.com/srtm30m). The 30m SRTM DEM was used to characterize the study area and deal with topography challenges to the classification.

2.3.4. National Irrigation boundaries

National irrigation systems (NIS) are large and medium schemes operated and maintained by National Irrigation Administration (NIA), the Philippines, providing irrigation service for rice-planted farmers. The irrigation boundaries (2011) and water release dates can be used to characterize the study area and analyse the classification map.

2.4. Field data

Field survey including site observations and farm interviews was conducted to help interpret the SAR images and validate the classifiers.

2.4.1. Sampling design

The aim of the sampling was to obtain field observations of rice cropping patterns practiced in the surveyed sites, following farm interviews of cropping practices by farmers.

Considering time and budget limitations, a purposive sampling method was adopted to collect field data from specific field locations and farmers. A three-stage sampling, developed earlier by the International Rice Research Institute (IRRI), was used with the province as the domain, municipality as the primary sampling unit, village as the secondary sampling unit and farm household as the tertiary sampling unit.

The municipalities were selected based on the Central Luzon Loop Survey (2015-2016) data (CLLS) and the farmer's selection was based on the MISTIG farmer survey (2013-14) data (MISTIG).

Selection of municipalities

- For this study, in order to collect particular information per cropping pattern, purposive sampling was used to select field locations among eight municipalities in Nueva Ecija and three municipalities in Tarlac province. Based on CLLS data as shown in Table 2.3, the number of municipalities selected per province was proportional to the rice area in the province. Santa Rosa was selected because it had the biggest area for rice-rice cropping pattern, likewise, Talugtog was chosen because rice-fallow was the dominant one. In this way, six municipalities were selected including Bongabong, Santa Rosa, Talugtog, Aliaga in Nueva Ecija and La Paz, Tarlac city in Tarlac. These municipalities were chosen to represent the diversity of cropping patterns across the study area.

Table 2.3 The area of cropping patterns in the eleven municipalities of Nueva Ecija and Tarlac from CLLS (shaded cells are selected municipalities in this study)

	Area (ha)	% Share in area							
		Rice cultivation					Non-rice cultivation		
		WS	Rice	Rice	Rice	Fallow	Nonrice	Nonrice	Nonrice	Fallow
		DS	Rice	Fallow	Nonrice	Rice	Rice	Nonrice	Fallow	Nonrice
Nueva Ecija	870		76	17	4	1	0	1	0	1
Aliaga	104		86	9	2	3	0	1	0	0
Bongabong	79		40	16	37	0	0	3	0	3
Guimba	121		71	26	1	1	0	0	0	0
Llanera	107		84	13	3	0	0	0	0	0
Munoz City	90		89	7	0	3	0	1	0	0
Santa Rosa	155		96	3	1	0	0	0	0	0
Talavera	114		90	3	1	3	0	1	0	1
Talugtog	100		33	64	0	3	0	0	0	0
Tarlac	395		51	15	6	24	1	3	0	1
La Paz	183		42	11	2	41	1	0	0	2
Tarlac city	103		51	33	9	2	0	2	1	0
Victoria	110		64	5	8	15	0	8	0	1
All	1265		68	16	5	8	1	1	0	1

Selection of villages and farmers

- Purposive sampling method also was employed to select particular villages and farmers for each municipality based on MISTIG farmer survey data. The selection was discussed with other colleagues to ensure maximum farm interviews and field observations during the fieldwork. 15 villages were selected from six municipalities across the study area as shown in Table 2.4. At least six farmers were chosen from each village to ensure different cropping patterns practiced as shown in Appendix II.

Table 2.4 Villages selected for sampling in each municipality

Province	**Municipality**	**number of rural villages**	**Selected villages for sampling**
Nueva Ecija			
	Bongabon	26	4 (Calaanan, Macabaklay, Pesa, Vega)
	Santa Rosa	32	2 (Berang, San Isidro)
	Talugtug	26	3 (Cabiangan, Alula, Villa Rosario)

Tarlac	Aliaga	8	2 (Pantoc, San Felipe)
	La Paz	19	2 (Macalong, Rizal)
	Tarlac city	35	2 (Villa Bacolor, San Manuel)

2.4.2. Field data collection

Field work was carried out between 24 September and 9 October in the Philippines, covering 2 provinces, 6 municipalities and 15 villages. 10 days were available for data collection including field observations and farmer interviews.

In summary, a total of 100 farmers were interviewed and 124 plots were measured. A minimum of 5 and a maximum of 13 sample plots were collected each day depending on distances and farmer availability and plot suitability. The distribution of visited farmers and measured plots are shown in Table 2.5.

Table 2.5 Summary of visited farmers and measured plots

Municipality	**Village**	**No. of HHID /farmers as samples**	**Visited farmers**	**Measured plots**
Bongabong	Macabaclay	7	7	10
	Pesa	9	6	8
	Vega	13	10	13
	Calanaan	6	5	5
Talugtug	Villa Rosario	18	10	11
	Alula	7	6	6
	Cabiangan	9	6	7
Tarlac City	Villa Bacolor	9	8	9
	San Manuel	6	6	7
La Paz	Macalong	8	6	10
	Rizal	7	6	7
Santa Rosa	Berang	6	6	7
	San Isidro	7	6	10
Aliaga	Pantoc	11	6	8
	San Felipe	10	6	6
Total		133	100	124

Regarding cropping pattern, rice-rice was the most common cropping sequence; Some farmers practised 3 crops in one year, 2 crops (rice, mungbean) in DS, 1 crop (rice) in WS; Some plots were fallow due to flooding by underground water in the WS or lack of water in DS. Apart from rice crop, farmers also planted other crops such as maize, onion, okra in DS. Six cropping patterns (DS-WS) were found in the survey, including rice-rice, rice-fallow, fallow-rice, other-rice, rice-other, and rice-other-rice. The distribution of different cropping patterns is shown in Table 2.6.

Table 2.6 The distribution of different cropping pattern in the fieldwork

Dry-Wet	Plots	Percentage
Rice-Rice	77	62%
Rice-Fallow	7	6%
Fallow-Rice	8	6%
Other-Rice	27	22%
Rice-Other	1	1%
Rice-Other-Rice	4	3%
Total	124	100%

Field observations were recorded including: (1) field corner coordinates and GPS tracks, (2) soil condition, (3) field sketch and (4) rice plant height. Crop growth stage dates for each season were recorded from farmer interviews according to the questionnaire, including questions on: (1) crop type, (2) crop number, (3) land preparation date, (4) flooding date, (5) harvesting date, and (6) maturity duration (see Appendix I). To achieve that, appropriate equipment was needed to conduct the field survey. Table 2.7 shows the list of equipment and their function.

Table 2.7 Equipment and their function for the fieldwork

Equipment	Function
Mobile GPS: HP 4700 IPAQ + ArcPad and Garmin eTrex 30(x)	To record the location and boundary of rice fields for training and validation purposes.
Questionnaire sets (paper sheet and clipboard)	A list of questions related to the rice field and planting practice, to get the information from the farmers.
Camera	To take pictures from rice fields samples
Rubber shoes	To ensure safety in the rice fields

Depending on vehicle availability, two villages could be reached per day in the first week and one village was visited per day in the second week (see Appendix III). Considering the rice-based cropping pattern and SAR imagery spatial resolution, only farmers who planted rice were interviewed and only plot areas that were more than 0.5 hectares were measured.

During the survey, we measured the rice field after the farmer interviews so that we could better understand the field conditions. In the interview, the farmers were usually gathered in the Barangay (village) hall where we could interview them in the hall or alternatively we visited the farmers' houses one by one. Two questionnaires were used to ask the prepared questions. For crop calendar, the *n*th week of the month was recorded if the farmers couldn't remember the exact dates, such as 1st week of November for land preparation. Once we finished the interview, we requested farmers to take us to their field where we could recognize the exact field boundary. The farmer interviews and field measurements are shown in Figure 2.5.

Farmer interview

(a): farmer interview in the Barangay hall

(b): farmer interview in the farmer's house

(a)

(b)

Rice plots measurement

(c): draw field sketch guided by farmer

(d): record field corner GPS coordinates

(c)

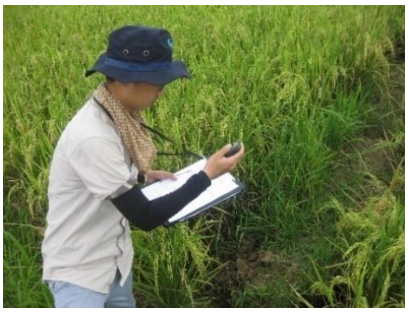

(d)

Figure 2.5 Farmer interviews and field measurements

In the field, most of the plots were irregular and consisted of more than four corners, which needed to be recorded by field tracking. Also, seedbeds, mango trees, huts and water pumps were observed inside the plots (see Figure 2.6), which needed to be excluded from the rice field boundary that we traced to avoid contaminating the real rice pixel signal. One rice field could have different cropping patterns, for example, in the dry season the field was divided into two parts, planted vegetable and rice separately, accordingly, and in these cases we divided the rice field into two plots and recorded the GPS points separately.

(a)

(b)

(c)

(d)

Figure 2.6 Excluded objects observed in the rice fields
(a) seedbed; (b) hut; (c) water pump; (d) mango tree

2.5. Software and tools

The software and tools which were used for data processing and analysis are shown in table 2.8.

Table 2.8 Software and tools used for data processing and analysis

Software/tools	Version	Purpose
ArcGIS	10.4.1	Cartography
Google Earth	7.1.8	Field digitization
SNAP Toolbox	5.0	SAR imagery processing
RStudio	3.4.2	Classifier training and validation; Image classification
Spectrum Extraction Tool	-	Mean value extraction
Microsoft Office Excel	2016	Statistical analysis
Microsoft Office Word	2016	Thesis writing

3. METHOD

The workflow of this study is shown in Figure 3.1. The main steps included field data processing, SAR data pre-processing, mean value extraction, polarization comparison and selection, non-rice area masking, parameters definition, temporal features selection, decision rules setting, classifiers validation and mapping.

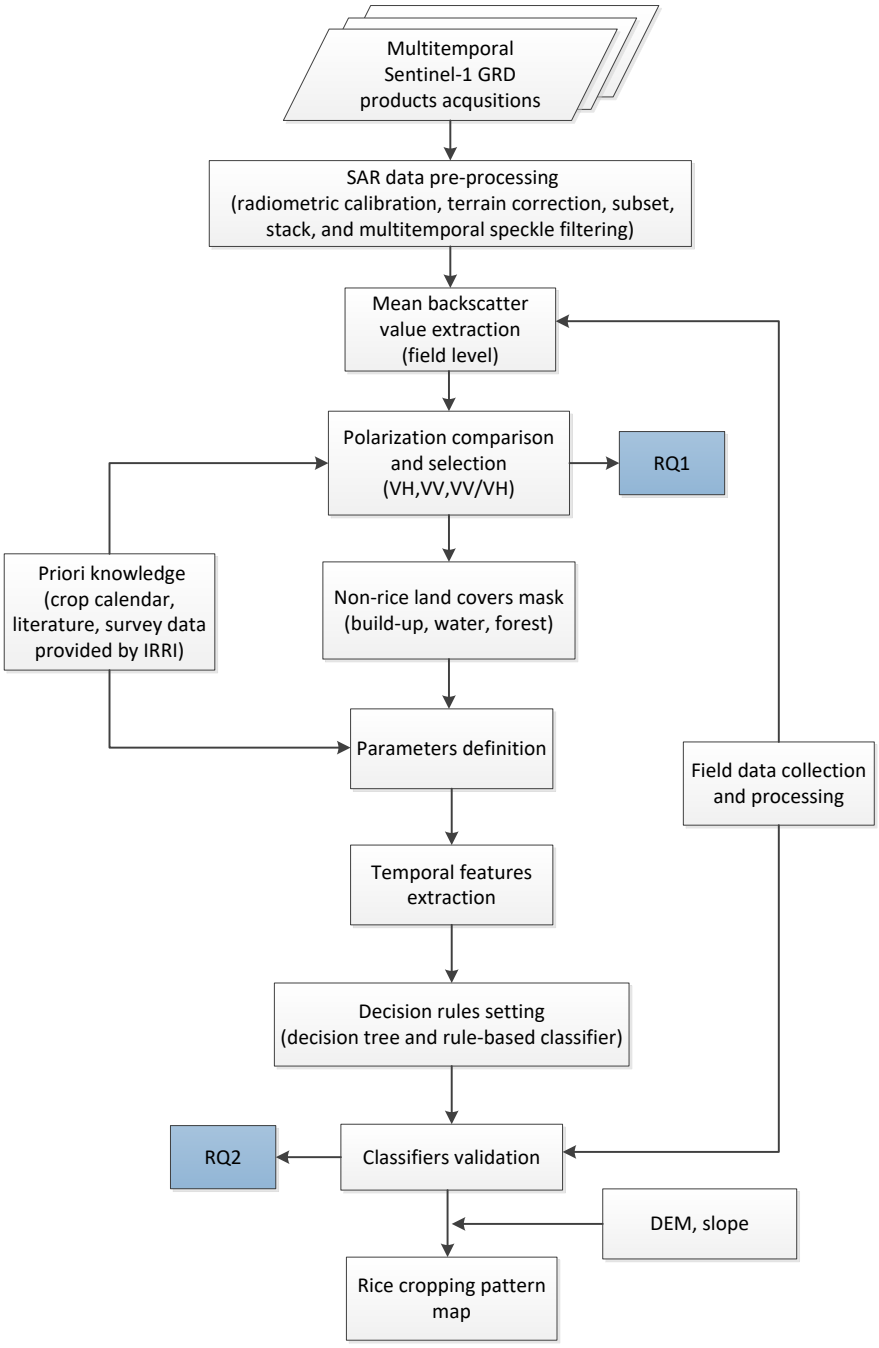

Figure 3.1 Methodological framework

3.1. Field data processing

To obtain a usable digital field dataset, we encoded the questionnaire into a digital version manually and imported the GPS points in Google Earth to digitize the rice plots. We visually excluded the non-rice objects based on field photos and remarks in the sketch such as seedbed, trees, and shed. Also, to ensure that the collected data, on cropping pattern, was representative for the study area, we compared it with the existing survey dataset from CLLS that covered the study area.

3.2. Sentinel-1 data pre-processing

SAR images from Sentinel-1A IW mode were acquired over the study area for the DS (2016-2017) and WS (2017) to identify different rice cropping pattern based on a temporal analysis of the backscatter coefficient (dB). The sets of the images in GRD format were processed using the Sentinel Application Platform (SNAP) toolbox developed by ESA. It is a common software for all Sentinel images and also an ideal tool for all remote sensing image processing and analysing (L. Mansaray et al., 2017). The GRD data were transformed into a terrain geocoded backscatter coefficient by following these processing steps:

(1) Slice assembly: Slice products can be combined to form an assembled Level-1 product with the same product characteristics covering the complete segment. The operator combines overlapping products into a single composite product.

(2) Apply orbit file, radiometric calibration and terrain correction: The orbit state vectors provided in the metadata of a SAR product are generally not accurate and can be refined with the precise orbit files which are available days-to-weeks after the generation of the product. The orbit file provides accurate satellite position and velocity information. Based on this information, the orbit state vectors in the abstract metadata of the product are updated. Geometric and radiometric correction is necessary for the comparison of SAR images acquired with different sensors or acquired from the same sensor but at different times, in different modes, or processed by different processors (Lemp & Koch, 2009). Range-Doppler equations (Meier, Frei, & Nüesch, 1993) were used to transform the two-dimensional coordinates of the slant range image to three-dimensional object coordinates in a cartographic reference system. Radiometric calibration was performed using a radar equation considering the scattering area, antenna gain patterns and range spread loss (Asilo et al., 2014).

(3) Land/Sea Mask: This operation was used to create spatial or spectral subsets by either ROI (region of interest) or imported shape file.

(4) Create stacks and time-series filtering: Stack one or more slave images with respect to a master image acquired with the same observation geometry. After stacking, the multitemporal filter can reduce the speckle noise on the time-series images both in spatial and temporal dimension. Refined Lee filter was applied to the stack images as it can preserve the spatial pattern of the object and give the better crop classification accuracy (Lavreniuk et al., 2017).

After these almost automatic processing steps, the corrected and normalized intensity values (DN) were generated for VH and VV separately. Then the ratio of VV and VH was created by simple band math: VV/VH (DN). The DN values were converted into backscatter coefficient ($\sigma°$) in the decibel scaling (dB) for the analysis and classification using the equation:

$$\sigma^0(dB) = 10\log_{10}(DN)$$

3.3. Mean backscatter value extraction (field level)

The data analysis was based on the field level. After excluding non-rice objects in the rice fields, we used the ENVI plug-in program called spectrum extraction tool developed by NRS Department of ITC (Faculty of Geo-Information Science and Earth Observation, University of Twente) to extract the mean DN value from time series SAR images for each polygon.

In order to remove the edge effect of the polygons and ensure that we extracted values from the real rice field pixels, we prepared two shape-files. One with the large polygons and then created a negative buffer of one-pixel size (-20m). And the other one with small polygons, those that either width or length was less than 3 pixels. In this way, we ran the program twice and got all the mean DN signatures out.

3.4. Polarization comparison and selection

Two different polarizations, VH and VV, and the band ratio (VV/VH) were compared based on the temporal evolution of the backscatter coefficient over the sample plots. The comparison included the following three steps:

(1) Backscatter coefficient extraction at land preparation and crop growth stages: We described the relationship among farming practice, crop calendar, and SAR acquisition timing. For each plot, based on the relation, the backscatter coefficient was selected from a single SAR acquisition that coincides with the timing of each farming event.

(2) Significance test: For rice and other crops (maize, onion, okra), they had same three events: land preparation (LP), crop establishment (CE) and harvest (HA). For each of the events (LP, CE, HA), the extracted backscatter coefficients were used to calculate the significant difference between rice and others.

(3) Real rice growth cycle examination: this last step was to check the sensitivity of polarization or band ratio to the rice growth. The sensitivity was evaluated by looking at the coincidence between temporal evolution and the rice growth stages.

We selected the polarization or ratio that provided the most promising significance for discriminating different crops at specific growth stages as well as representing the real rice growth cycle.

3.5. Non-rice land covers mask

The rice cropping patterns detection and classification were applied for rice fields. Other land covers such as built-up, water and forest potentially affected the rice signals, so we generated a non-rice land cover mask to minimize their potential impacts.

Stable water tends to have consistently low backscatter value throughout the year. Since the flooding/transplanting period was temporary, flooded rice pixels were expected to have short period of low values. We excluded water bodies where the average σ° was lower than an expected threshold. Evergreen forest and built-up tend to have consistently high backscatter values throughout the year, while rice pixels tend to have high values only in a few periods, mostly prior to harvesting. We masked out forest and settlements where the average σ° was higher than an expected threshold.

3.6. Parameters definition and temporal features extraction

After field data analysis and polarization selection, we defined the threshold parameters and corresponding temporal features to classify different cropping patterns.

Threshold parameters were defined from an agronomic perspective, which also required a priori knowledge of crop calendar, maturity duration, crop practices from field survey as well as the SAR temporal behaviours. The temporal signature is frequency and polarization dependent and also depends on the crop establishment method (Nelson et al., 2014). This implies that the parameters for the rules setting may need to be adapted according to the study area, crop practices, and crop calendar.

For this study, considering the distribution of crops for each season and processing time, we divided the cropping pattern into DS pattern (Nov 2016-May 2017) and WS pattern (June 2017 – Oct 2017). Accordingly, we needed to set threshold parameters for each season separately. The defined parameters and the corresponding temporal features for maximum discrimination among different crops or fallow are shown in Table 3.1. We defined five parameters (P1-P5) in DS and one parameter(P6) in WS.

Table 3.1 Parameters and corresponding temporal features used for the discrimination of rice, other crops and fallow.

Season	**Parameter code**	**Parameter**	**Description**	**Relationship between**	
				Temporal features	**Growth cycle**
Dry	P1	SoS (dB)	Start of season	*a*	dry flooding/crop establishment
Dry	P2	PoS (dB)	Peak of season	*b*	dry flooding/crop establishment to the end of reproductive phase
Dry	P3	Span of SoS to PoS (dB)	Amplitude from start to peak season	*c*	-
Dry	P4	Mean of post-harvest (dB)	Average backscatter of harvested to next land preparation	*d*	After harvest and before land preparation
Dry	P5	Growth duration from SoS to PoS (days)	Number of days from start to peak season	*e*	-
Wet	P6	Mean of SoS to reproductive phase (dB)	Average backscatter of SoS to reproductive phase	*f*	wet flooding/crop establishment to the end of the reproductive phase

Table 3.2 shows the criteria to generate temporal features from each temporal signature. For temporal signatures of each sample plot, in DS, we calculated *a*) minimum value in the period of dry flooding/crop establishment, *b*) maximum value in the period of SoS to reproductive phase, *c*) range of maximum and minimum value, *d*) the mean value in the period of post-harvest and *e*) growth duration from SoS to PoS. In WS, we calculate *f*) the mean value from wet flooding/crop establishment to reproductive phase. These six statistics, which we called temporal features, concisely characterized the key information of observed field signatures to distinguish rice, others and fallow, and each one related directly to one parameter.

Table 3.2 The criteria to generate temporal features from each temporal signature

Temporal features	Relationship between temporal signatures at specific timing	Specific timing
a	minimum value of each signature	Period of dry flooding/crop establishment (T1)
b	maximum value of each signature	Period of SoS to the end of reproductive phase(T2)
c	range of maximum and minimum value	-
d	mean value of each signature	Period of post-harvest(T3)
e	growth duration of each signature (number of images*temporal resolution)	-
f	mean value of each signature	Period of wet flooding/crop establishment(T4) to the end of reproductive phase(T2)

3.7. Decision rules setting

Decision tree and rule-based classifiers employed the same parameters and temporal features in section 3.6 to generate the rules respectively.

3.7.1. Decision tree classifier

A decision tree is defined as a classification procedure by recursively partitioning a dataset into smaller subdivisions as a function of the input feature space (Friedl & Brodley, 1997). The classification structure is explicit and therefore easily interpretable. Because of that, we can examine the tree structure and identify the principal features that could distinguish classes from one another at each step.

The decision tree classifier was conducted with the "tree" package (version 1.0-37) in R Studio. The package was developed by Ripley (1996) based on the CART algorithm proposed by Breiman et al. (1984). The package incorporates a type of decision tree in which the decision boundaries at each node of the tree are defined by a single feature of the input data (Swain & Hauska, 1977). To determine the specific values of decision boundary, a Boolean test is applied at each internal node:

$$X_i > b$$

where X_i is a feature in the training data and b is a threshold in the observed range of X_i. b is estimated by maximizing dissimilarity in the descent nodes. Cross-validation is used to estimate the performance (overall number of misclassifications) of the tree model, avoiding overfitting the training data.

According to the agronomic parameters described in table 3.2, in DS, five temporal features (*a*-*e*) were extracted from the temporal signatures of each training plot to discriminate rice, others and dry fallow, and one temporal feature (*f*) in WS to differentiate rice and wet fallow. We used the temporal features and corresponding class labels as input to generate the decision rules and splitting thresholds for DS and WS separately.

3.7.2. Rule-based classifier and threshold selection

The rule-based cropping pattern detection algorithm was developed to classify multitemporal C-band σ° images, which follows Nelson et al. (2014) and Asilo et al. (2014). The multitemporal stack of terrain-geocoded σ° images in DS and WS was input to the classifier separately in R Studio. Figure 3.2 gives an

overview of the developed rule-based discrimination algorithm. Details are explained below.

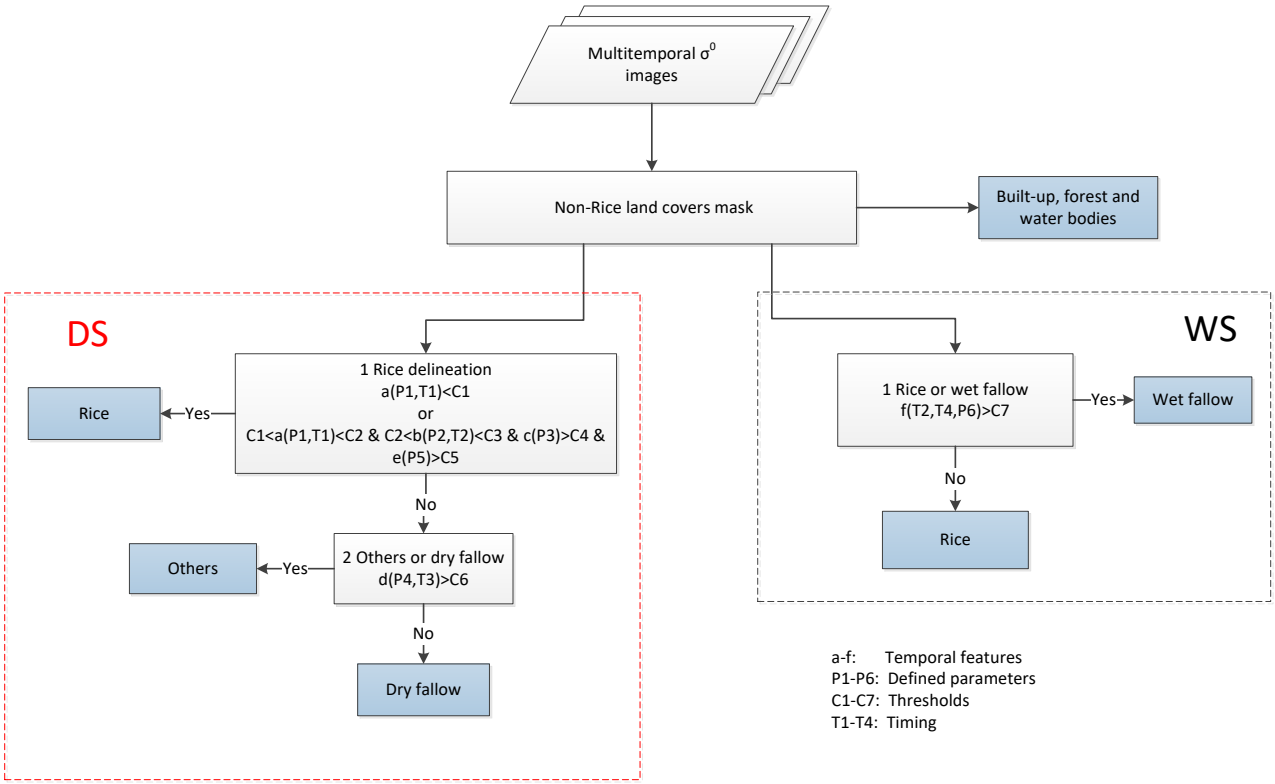

Figure 3.2 Rule-based cropping pattern discrimination algorithm for multitemporal C-band σ° in DS and WS

The rule-based classifier was developed as the following and the rules were applied to the temporal signature for each pixel:

After masking out non-rice land covers, the remaining pixels are either rice, others or fallow. Each pixel consists of six temporal features extracted from the temporal signatures: *a, b, c, d, e, f.*

In DS, the first rule is rice delineation. We look for the lowest value (*a*) that occurs in the dry flooding/crop establishment period (T1), this marks the start of crop growing cycle (SoS) (P1). For the detected SoS of the pixel, we apply two conditions for rice delineation:

1) Certain rice condition: if *a* is lower than the expected threshold (C1), the pixel is classified as rice, or

2) Uncertain rice condition: if *a* falls between threshold C1 and C2, during the period of SoS to reproductive phase (T2), we look for a rapid increase in biomass that confirms that rice is grown. The parameters used to detect rice growth are PoS (P2), a span of SoS to PoS (P3), and growth duration from SoS to PoS (P5), and the corresponding temporal features are b, c and e respectively. Any pixel that meets all the three judgments is labelled as rice: C2 < *b* <C3 and *c* > C4 and *e* > C5. This helps distinguish rice from other crops and fallow.

If the pixel meets none of the above conditions, it should be either other or fallow, then we apply the second rule to distinguish other from fallow. After harvesting (T3), the remaining dry crop biomass in the field is expected to exhibit higher backscatter than fallow land. We set the mean of post-harvest (*d*) to

distinguish others from fallow. If *d* is higher than the expected threshold C6, the pixel is labelled as others, otherwise, fallow.

In WS, the rule is to discriminate rice from wet fallow. For rice, the SoS occurs in the wet flooding/crop establishment period (T4). Due to increasing water content of bare soil in the wet season, the backscatter coefficient of wet fallow is expectedly higher than rice crop. We set the mean value (*f*) from SoS to reproductive phase (P6), in the period of T2, to make discrimination between rice and wet fallow. If *f* is higher than the expected threshold (C7), the pixel is labelled as wet fallow, otherwise, rice.

The timing of T1-T4 was estimated based on crop calendar and duration between growth stages, and threshold selection of C1-C7 was guided by the temporal backscatter coefficients extracted from training plots.

3.8. Classifiers validation

We used a random selection of 60% of field data to train the classifiers and generate classification rules. The remaining 40% were used to validate the classifiers. A standard confusion matrix was applied to the decision tree and rule-based classifier respectively. The overall accuracy and the kappa values were recorded.

3.9. Rice cropping pattern map

Based on the validation results, we applied the best performing classifier to the time series SAR data to generate DS pattern and WS pattern maps. As shown in Figure 3.3, the combination of these two consecutive maps resulted in an initial cropping pattern map over one year.

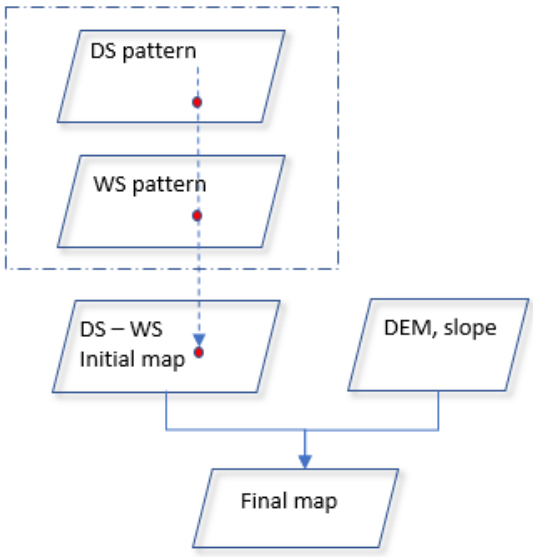

Figure 3.3 Diagram showing the data and procedures involved in generation of annual cropping pattern map

Almost all of the rice area in the study site lies in the plains. Xiao et al. (2006) indicated that rice was situated at elevations no more than 2000 m or with a slope less than 2°. Therefore, we applied 30m SRTM Digital Elevation Model (DEM) to generate an elevation mask and used it to exclude those areas above 2000 m or with a slope greater than 2°.

4. RESULTS

4.1. Field data processing

After the field work, we manually encoded the questionnaire to a digital version. We set the proper column name and consistent row code style for all 124 plots to ensure readability and coherence. We imported the GPS points in the Google Earth to digitize the rice plots, and visually excluded the non-rice objects based on the remarks in the sketch such as seedbed, trees, and huts. Figure 4.1 shows the distribution of digitized plots across the study area. Next, we joined the polygons and tables in the ArcMap to produce the entire field data shapefile.

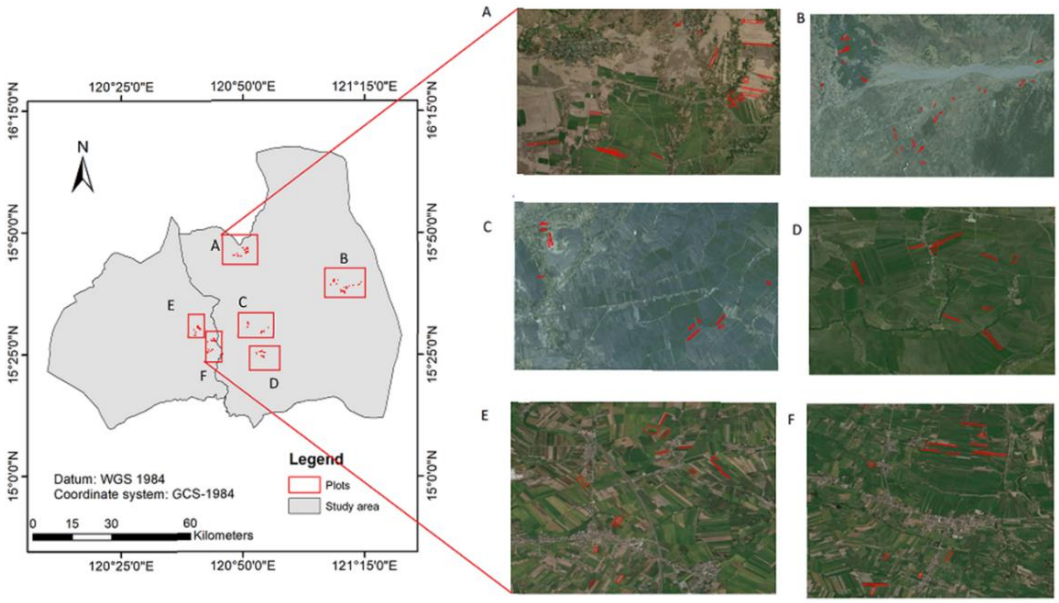

Figure 4.1 Distribution of visited plots across the study area

To assess the representativeness of the cropping patterns summarized from field work, we compared it with the existing survey dataset CLLS that covers the study area. We extracted 55 famers with 94 plots located in the study area and summarized the cropping pattern as shown in Table 4.1. From the comparison with the existing datasets, the field data matched CLLS to some extent and can be representative of the study area.

Table 4.1 Summary statistics (94 samples) of different cropping patterns from CLLS

Dry-Wet	Samples	Percentage
Rice-Rice	57	61%
Rice-Fallow	10	11%
Fallow-Rice	7	7%
Other-Rice	15	16%
Other patterns	5	5%
Total	94	100%

Due to the limited plots of rice-other and rice-other-rice, we only considered rice-rice, other-rice, rice-fallow and fallow-rice as the major rice cropping patterns practised in the study area. We used 60% of the

field data for training the classifier and the remaining data for accuracy assessment. Table 4.2 shows the number of plots used for training and validation per cropping pattern.

Table 4.2 Number of plots used for training and validation per rice cropping pattern

Cropping pattern	Total plots	Number of plots for training	Number of plots for validation
Rice-Rice	77	46	31
Other-Rice	27	16	11
Rice-Fallow	7	4	3
Fallow-Rice	8	5	3

4.2. Polarization comparison and selection

In order to analyse the dry season (DS) and wet season (WS) patterns separately, the training and validation sets (see table 4.2) were divided into DS patterns and WS patterns. The number of training and validation plots for each season is shown in Table 4.3.

Table 4.3 Number of training and validation plots for DS and WS

Season	Crop or fallow	Training samples	Validation samples
DS	Rice	50	34
	Others	16	11
	Dry fallow	5	3
WS	Rice	67	45
	Wet fallow	4	3

Table 4.4 describes the relation between farming events, crop calendar and SAR acquisitions, and the backscatter coefficient was extracted from the SAR acquisition that coincided with land preparation (LP), crop establishment (CE), and harvest (HA) of rice and other crops at VH, VV and VV/VH.

Table 4.4 Relationship among farming practice, crop calendar, and SAR acquisition in dry and wet season (LP: land preparation; FL: flooding; CE: crop establishment; HA: harvest)

	Dry season							Wet season			
Crop	Rice				Others (maize, onion, okra)			Rice			
Farming practice	LP	FL	CE	HA	LP	CE	HA	LP	FL	CE	HA
Crop calendar	Nov -Jan	Nov-Jan	Nov-Jan	Feb-Apr	Nov-Jan	Nov-Jan	Feb-Apr	Jun-Jul	Jun-Aug	Jun-Aug	Sep-Nov
SAR acquisition	1 Nov 13Nov 25Nov 7 Dec 19Dec 31Dec 12Jan	1 Nov 13Nov 25Nov 7 Dec 19Dec 31Dec 12 Jan	1 Nov 13Nov 25Nov 7 Dec 19Dec 31Dec 12 Jan 24 Jan	5Feb 17Feb 1Mar 13Mar 25Mar 6Apr 18Apr 30Apr	1 Nov 13Nov 25Nov 7 Dec 19Dec 31Dec 12 Jan	1 Nov 13Nov 25Nov 7 Dec 19Dec 31Dec 12 Jan 24 Jan	5Feb 17Feb 1Mar 13Mar 25Mar 6Apr 18Apr 30Apr	5Jun 29Jun 11Jul 23Jul	5Jun 29Jun 11Jul 23Jul 4Aug	5Jun 29Jun 11Jul 23Jul 4Aug 16Aug	9Sep 21Sep 3Oct 15Oct 27Oct 1Nov 13Nov

The backscatter values of other crops such as maize (7 samples), okra (5 samples), and onion (12 samples) showed little difference between them during land preparation (LP) and crop growth stages (CE, HA) (see Appendix IV). Therefore, maize, okra, and onion were combined into one group "Others" for further analysis. Figure 4.2 shows the range of backscatter values extracted from Sentinel-1A data for Rice and Others plots, grouped by LP, CE, and HA for VV and VH polarizations and the VV/VH ratio.

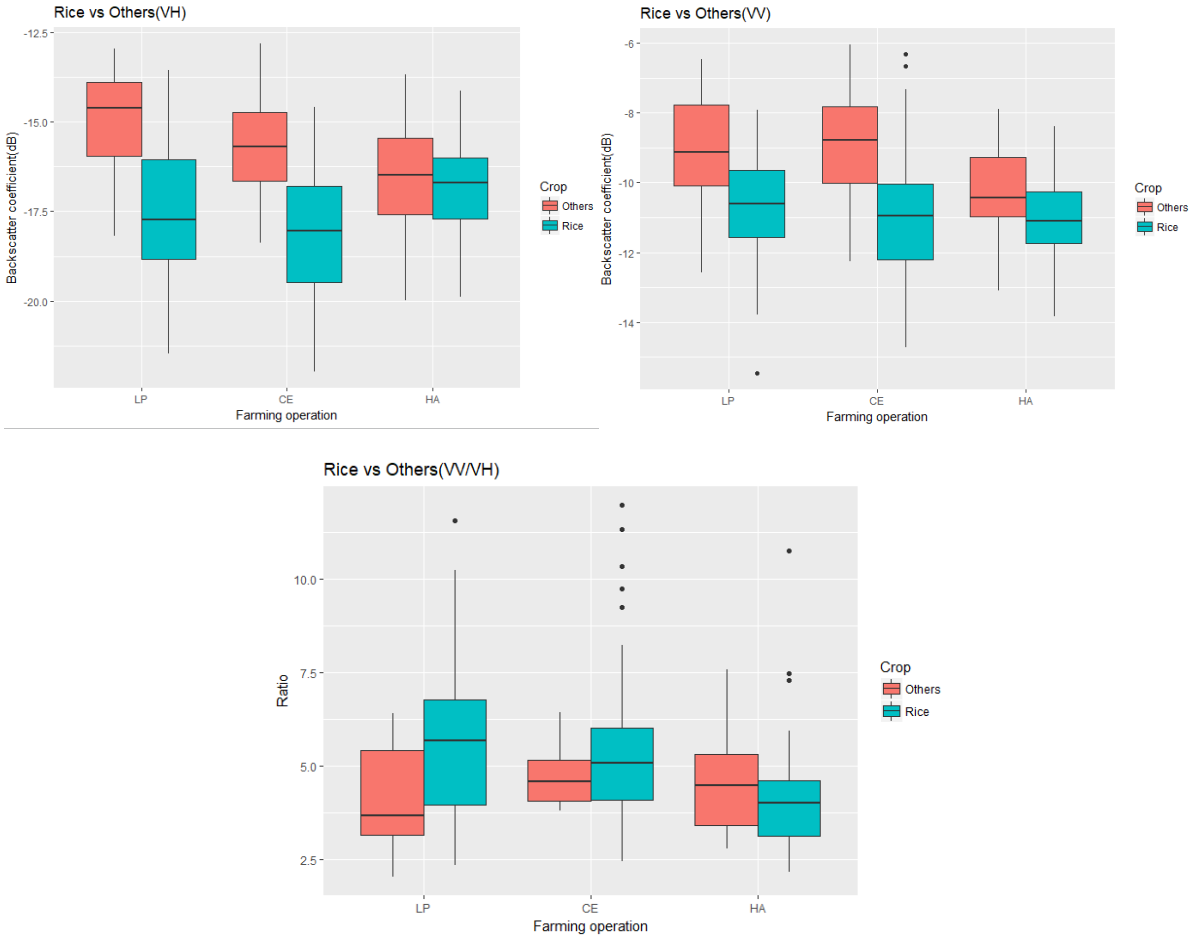

Figure 4.2 Boxplots of the backscatter coefficient derived from Sentinel-1A for LP, CE and HA at the monitored Rice (50 samples) and Others (16 samples) plots for VH (**upper left**), VV (**upper right**) and VV/VH (**bottom**). The black dots represent the outliers, the thick horizontal black line in the middle of the box is the median, the lower half of the box is the 25th percentile and the upper half is the 75th percentile, and the extent of the solid lines represents the minimum and maximum. Note the different scale and unit in the vertical axes.

For VH, VV and VV/VH, we applied single-factor ANOVA to test significant difference between Rice and Others at LP, CE, and HA respectively. The significance test results are shown in Table 4.5.

Table 4.5 P-values of ANOVA tests between Rice and Others at LP, CE, and HA

Polarization or band ratio	**Farming operation**	**P-value**
VH	LP	1.8411E-07***
	CE	2.1762E-06***
	HA	0.2204
VV	LP	0.0006***

	CE	0.0003***
	HA	0.0144*
VV/VH	LP	0.0066**
	CE	0.1296
	HA	0.3570

(* statistically significant at 0.05 level; ** statistically significant at 0.01 level; *** statistically significant at 0.001 level)

From the above table, we can see that both VH and VV showed promising significance at land preparation and crop establishment stage. Next, we examined whether VH or VV could represent the real rice growth cycle.

Based on farmer interview and expert knowledge, we extracted backscatter values from VH and VV at land preparation and each rice growth stage, grouped by land preparation (LP), flooding (FL), crop establishment (CE), tillering (TL), stem elongation (SE), heading to flowering (HD), maturity (MT) and harvest (HA) as shown in Figure 4.3.

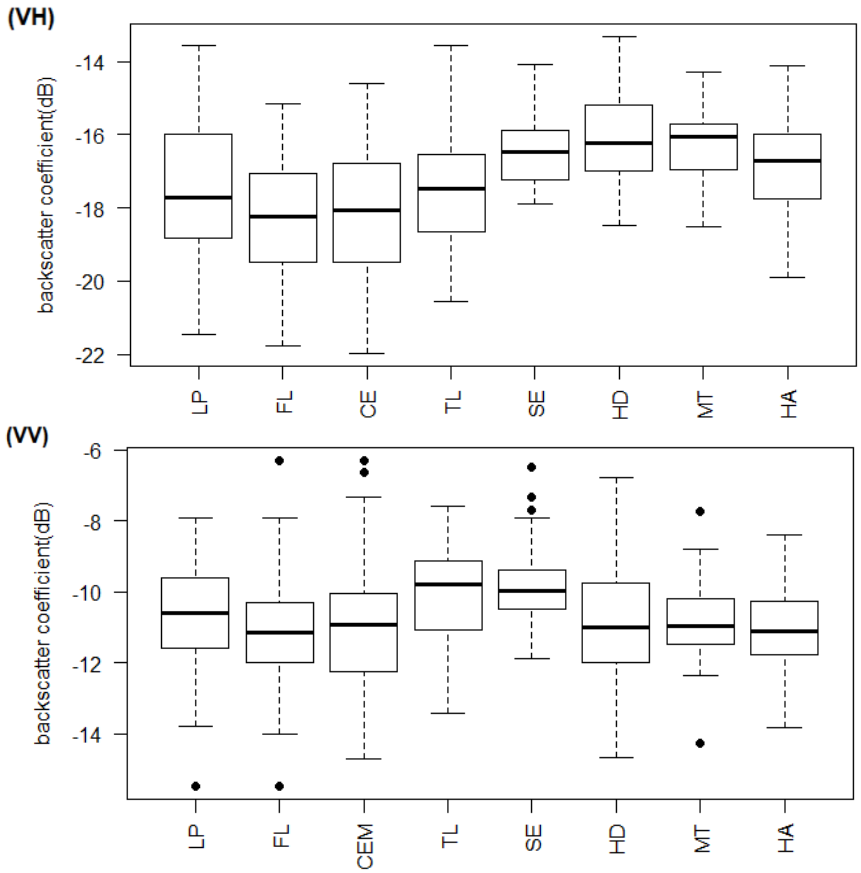

Figure 4.3 Boxplots of the backscatter coefficient derived from VH (**top**) and VV (**bottom**) for each land preparation and growth stage at the monitored rice (50 samples) plots. The black dots represent the outliers, the thick horizontal black line in the middle of the box is the median, the lower half of the box is the 25th percentile and the upper half is the 75th percentile, and the extent of dashed lines represent the minimum and maximum. Note the different scale in the vertical axes.

In the above boxplots, VH had a larger dynamic range of backscatter than VV through the rice growth cycle. VH showed consistent increase form tillering to heading as opposed to VV.

As an example, Figure 4.4 shows the backscatter dynamic of one rice plot at the VH and VV polarizations of Sentinel-1A. VH polarization showed the most consistent increase in paddy rice backscatter, increasing from crop establishment to the end of reproductive phase, however, VV polarization exhibited sudden decrease from tillering to stem elongation and increase again at heading stage. Rosenthal et al. (1985) also indicated that crop biomass and height were correlated positively with C-cross (VH or HV) backscattering coefficients at high incident angles. We could consider the maximum backscattering values during the crop growth cycle as the peak of crop biomass.

In summary, VH polarization showed a significant difference in land preparation and crop establishment stage as well as represented the real rice growth cycle, so we selected the VH polarization for further analysis.

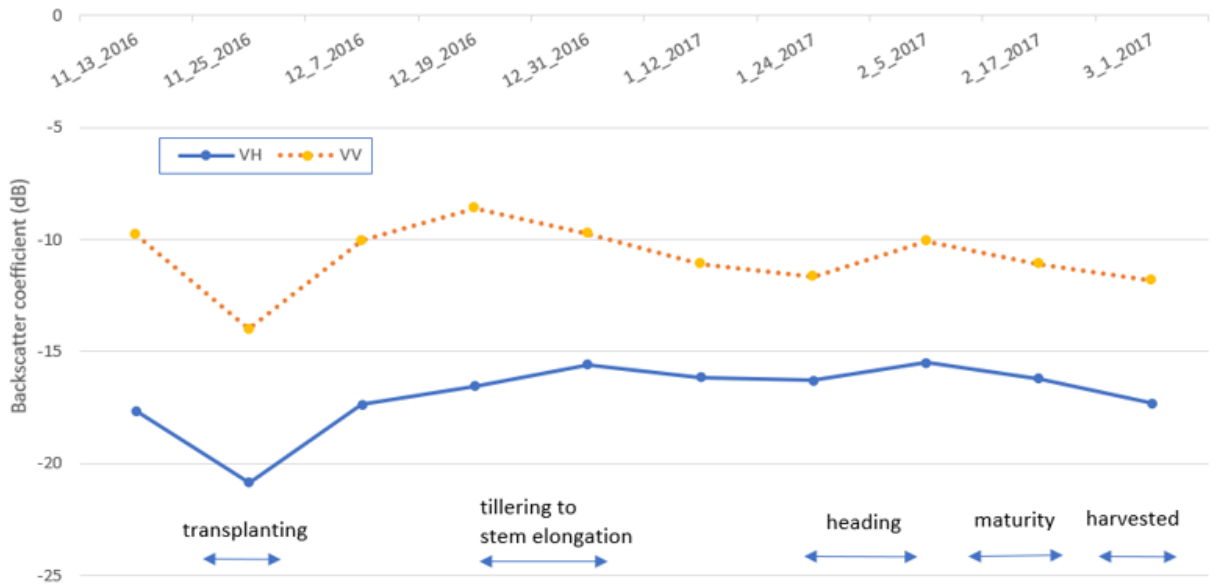

Figure 4.4 Backscatter dynamic of the rice plot at the VH and VV polarizations

4.3. Non-rice land covers mask

We masked out other land covers to minimize the impacts on the rice cropping patterns classification. We draw the same number of homogenous sample plots in the Google Earth for each other land cover (stable water, built-up and forest) and extracted the average DN values from the temporal signatures for each sample using the spectrum extraction tool.

Figure 4.5 shows the backscatter dynamic of different land covers for selected sample plots at VH polarization. Samples in DS are shown for water bodies, built-up, forest, rice, others, and dry fallow in the top portion, while water bodies, built-up, forest, rice, wet fallow in WS are shown in the lower portion.

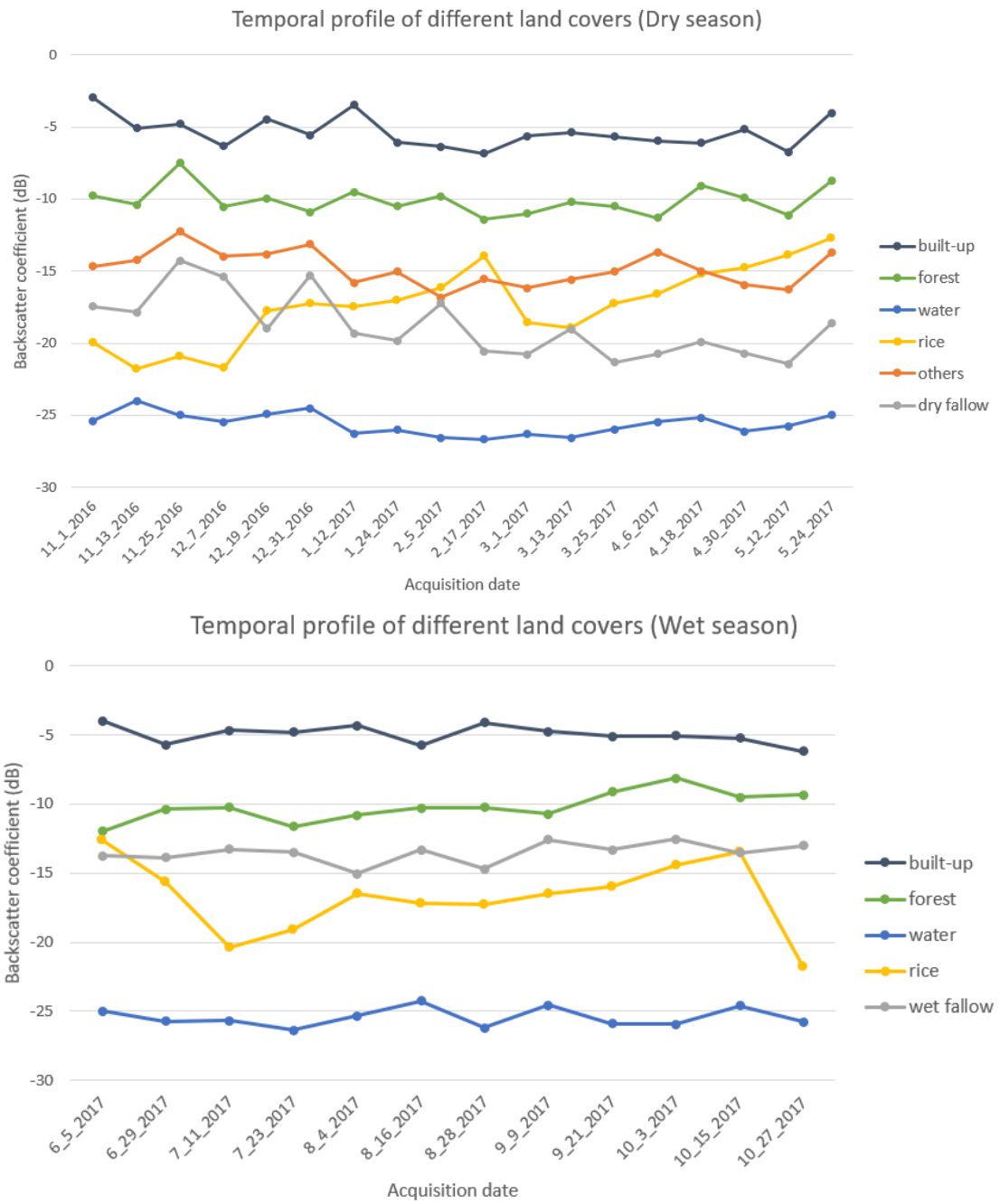

Figure 4.5 Backscatter dynamic of different land covers for selected sample plots in DS (**top**) and WS (**bottom**) at VH polarization

From the above graphs, in both seasons, water bodies have a consistently very low to low dB value and urban areas showed consistently higher backscatter, whereas forest with consistently dense vegetation over time was characterized by a consistent medium to high backscatter coefficient. Rice fields were usually flooded with water prior to crop establishment(Boschetti et al., 2014), which showed lower SAR backscatter compared to other crops, maize, for example, was not inundated at this stage(Asilo et al., 2014).

In the DS, the temporal profile of dry fallow land showed large fluctuations during the early season, and lower backscatter values in May compared to rice and other crops, while wet fallow exhibited relatively

consistent higher values than rice crop. The different behaviours between dry fallow and wet fallow could be attributed to soil moisture increase in WS.

In short, stable water, built-up and forest presented distinct temporal patterns compared with different crops and fallow. Based on the temporal signatures throughout the year, we excluded water bodies where the average σ° was lower than -22 dB and masked out forest and settlement where the average σ° was higher than -13 dB.

4.4. Decision rules setting and threshold selection

4.4.1. Temporal features extraction

In DS, we discriminated between rice, others and dry fallow, whereas, only rice and wet fallow were present in the WS. Table 4.6 shows the classes and temporal features in each season. Temporal signatures were extracted for each training and validation plot and used to generate the six temporal features: 5 in DS and 1 in WS. The criteria in Table 3.3 were applied to extract the six temporal features from the signatures. The temporal features generated in both seasons for each site are provided in Appendix V.

Table 4.6 Temporal features and classes in DS and WS

Season	Classes	Temporal features
DS	Rice, others, dry fallow	*a, b, c, d, e*
WS	Rice, wet fallow	*f*

T1, T2, T3, and T4 were estimated based on farmer interviews and expert knowledge. T1 reflected the period where the flooding/crop establishment occurred in DS. From the farmer interviews, most of the rice fields in dry season were flooded or established from November to January.

T2 restricted the number of days between the start of the season and the reproductive phase. 90 days was a suitable cut-off to cover the vegetative and reproductive phases no matter if the crop establishment method was direct seeding or transplanting.

T3 represented the post-harvest duration in DS. In the field survey, most of the crop fields were harvested before April and the next season started in June, so the one month in May could be regarded as the post-harvest period.

T4 reflected the period where the flooding/crop establishment occurred in WS. From the farmer interviews, most of the rice fields in wet season were flooded or established between June and August.

4.4.2. Decision tree classifier

The classes and corresponding temporal features were input to the "tree" package in R to generate decision trees and thresholds. In both seasons, 10-fold cross-validation was performed to avoid overfitting. In DS, the classifier identified 3 important features (*a, b* and *e*) out of 5 to classify rice, others and dry fallow. In WS, the one feature (*f*) is used to discriminate rice from wet fallow. The rules and thresholds for each season are shown in Figure 4.6.

Figure 4.6 Decision rules and thresholds generated for DS (**left**) and WS (**right**)

4.4.3. Rule-based classifier and threshold selection

Temporal features of each training plots were used as input to train the rule-based classifier. Expert knowledge and the temporal backscatter signatures were used to guide the threshold selection. Table 4.7 shows the temporal features and the corresponding thresholds selected for the rule-based classifier in DS and WS.

Since C-band σ° increases rapidly from tillering until it reaches a maximum value between stem elongation and the end of a reproductive phase in the temporal signatures, therefore, the minimum duration from SoS to PoS was held constant as 30 days.

Table 4.7 Thresholds selected for rule-based classifier in DS and WS

Season	Parameter	Temporal features	Relationship between thresholds
DS	SoS (dB)	*a*	<-21 or (-21, -17)
	PoS(dB)	*b*	(-17, -14)
	Span of SoS to PoS(dB)	*c*	>2.5
	Post-harvest(dB)	*d*	> -17
	Growth duration from SoS to PoS(days)	*e*	> 30
WS	Mean of SoS to end of reproductive phase	*f*	<-14

4.5. Classifiers validation

The validation datasets were used to validate the decision tree and rule-based classifiers. The predictive outputs were obtained for DS pattern and WS pattern separately and combined into the annual cropping pattern DS-WS. The standard confusion matrix was calculated using the actual cropping patterns and predictive outputs.

The rice, other crops and dry fallow were classified in the DS pattern, while rice and wet fallow were discriminated in the WS pattern. The combination of two patterns resulted in the annual cropping pattern (rice-rice, rice-fallow, fallow-rice, other-rice). Table 4.8 shows the confusion matrix of the decision tree classifier and rule-based classifier respectively. The overall accuracy and kappa values were calculated from the confusion matrix and shown in Table 4.9.

Table 4.8 The confusion matrix of decision tree classifier (**up**) and rule-based classifier (**bottom**)

Decision tree		Actual				
		rice-rice	rice-fallow	fallow-rice	other-rice	Sum
Classified	rice-rice	29	0	2	7	38
	rice-fallow	0	3	0	0	3
	fallow-rice	0	0	0	0	0
	other-rice	2	0	1	4	7
	Sum	31	3	3	11	48

Rule-based		Actual				
		rice-rice	rice-fallow	fallow-rice	other-rice	Sum
Classified	rice-rice	29	0	2	4	35
	rice-fallow	0	3	0	0	3
	fallow-rice	1	0	1	0	2
	other-rice	1	0	0	7	8
	Sum	31	3	3	11	48

Table 4.9 The overall accuracy and kappa values for each classifier

Cropping patterns (rice-rice, other-rice, rice-fallow, fallow-rice)	**Classifier**	**Overall accuracy (%)**	**Kappa coefficient**
	Decision tree	75	0.45
	Rule-based	83	0.66

From the validation results, we concluded that the rule-based classifier outperformed the decision tree in terms of overall accuracy and kappa value.

4.6. Rice cropping pattern map

We applied the rules and thresholds in the rule-based classifier to the multitemporal σ° images to generate DS pattern and WS pattern map separately. The combination of these two consecutive maps resulted in an initial cropping pattern map (DS-WS) over one year as shown in Figure 4.7.

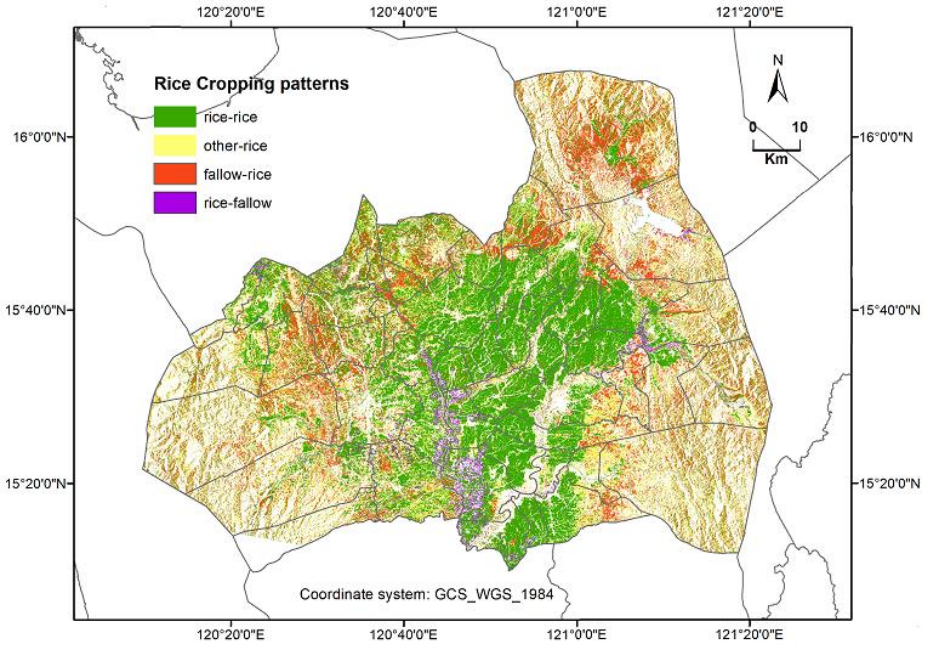

Figure 4.7 Rice cropping pattern obtained from rule-based classification of multitemporal Sentinel-1 images during the dry and wet season (DS-WS)

Due to terrain effect and noise, some misclassified isolated pixels or small regions of pixels existed in the classified map. This gave the output a "salt and pepper" or speckled appearance. To remove the terrain effect, we used the 30m SRTM Digital Elevation Model (DEM) to exclude those areas above 2000 m or with a slope greater than 2° (Xiao et al., 2006). To remove random noise, we used the 3x3 majority filter in ArcMap to smooth the classification map. Figure 4.8 shows the final classification map.

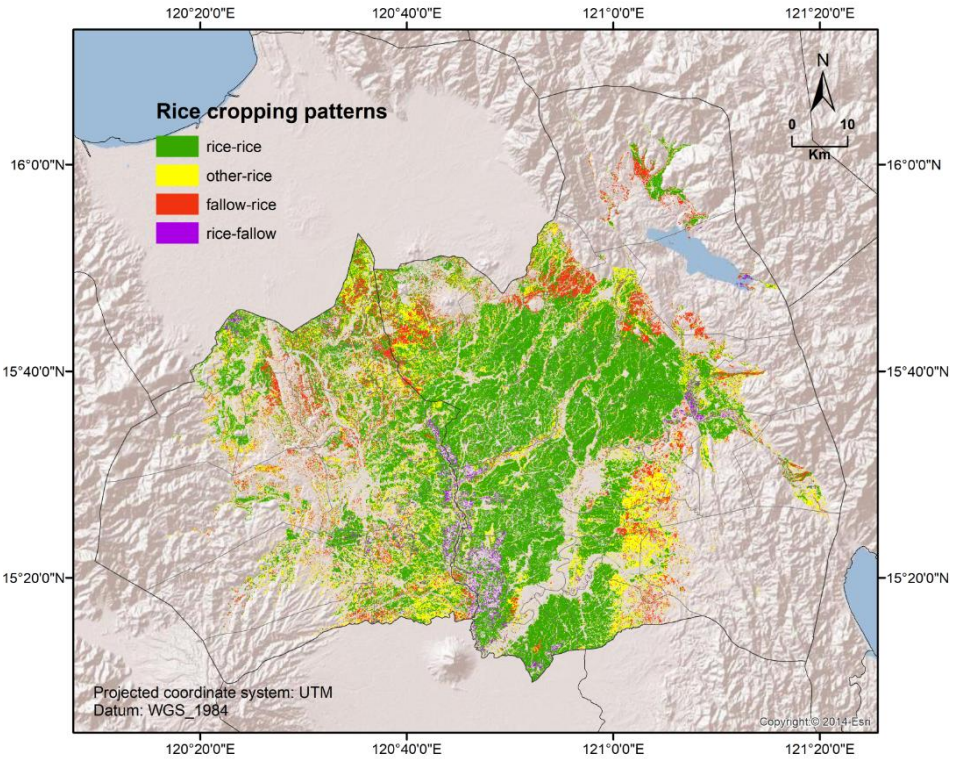

Figure 4.8 Rice cropping pattern in Nueva Ecija and Tarlac, Central Luzon, Philippines.
The map is obtained using rule-based classification of multitemporal Sentinel-1 images (2016-2017) and is corrected for topography.

5. DISCUSSION

In this study, we examined the potential of SAR time series data to detect where and what rice cropping patterns have been practised over large rice-planted areas in the Philippines. To explore the probability, we employed time series Sentinel-1 imagery and field survey data to identify the rice cropping patterns, involving: (1) determining the best polarization or band ratio to differentiate various rice cropping patterns; (2) comparing the performance of rule-based and decision tree classifiers in classifying different cropping patterns. The findings and limitations throughout the thesis have been discussed in the following subsections.

5.1. Findings in the field

Field observations and farmers interviews were carried out to determine the actual farming practices at the time of SAR acquisitions. As such the backscatters from temporal SAR signatures that coincided with the seasonal crop calendar and growth stages in the dry season (DS) and wet season (WS) were extracted.

The field survey was performed in Nueva Ecija and Tarlac provinces in which 100 farmers were interviewed and 120 rice plots were visited. The results of the survey revealed that the rice-rice rotation was the dominant cropping pattern practised by local farmers, followed by other-rice, fallow-rice and rice-fallow. In the national irrigation system (NIS) areas, farmers normally cultivated two crops of rice annually due to sufficient irrigation water throughout the year. Only one rice crop was cultivated during the WS in the remaining areas where water was insufficient, followed by fallow or a non-rice crop during the DS.

The annual crop establishment window in this region (for all crops, rice, maize, onion and okra) spanned several months with farmers establishing their crop anytime between November and January in the DS, and from June to August in the WS, though the peak planting months were December and June. The large range of the planting dates over the study area could be explained by different crop varieties, water release dates and individual farmer practices. From the analysis of the temporal backscatter of different crops, we considered the lowest backscatter at the flooding/planting stage as the primary condition to distinguish rice from other crops. This required adequate SAR observations to cover the dynamics in the crop establishment window that can capture the lowest backscatters at the start of the growing season (Mansaray et al., 2017).

Furthermore, we selected farmers based on the MISTIG survey data to ensure the diversity of cropping patterns. However, in the survey, some farmers changed their crop practices which were different from those recorded in MISTIG. For example, in the DS, some farmers cultivated rice crop instead of leaving the field unplanted because they recently bought new water pumps to pump irrigation water from underground or canals. In the village of Macabaclay, the irrigation canals were destroyed by the typhoon, thus most of famers changed rice to vegetables due to lack of water. Also, some farmers were not available during the survey so that we lost some sample plots practiced with specific cropping patterns (e.g. fallow-rice or rice-fallow). The practice changes, typhoons and unexpected absence of farmers accounted for the limited samples of fallow-rice and rice-fallow. This also implies that field work needs to be done every year due to crop practice changes by local farmers.

5.2. Findings in the results

5.2.1. Polarization comparison and selection

VH polarization outperformed VV in terms of sensitivity to rice growth and was thus utilized to classify different rice cropping patterns. VH signatures showed a consistent increase in backscatter from flooding/crop establishment to the end of the reproductive phase. However, the temporal signatures of VV channel presented a sudden decrease from tillering to stem elongation and increased again at heading stage. The decrease could be attributed to the significant attenuation by the vertical vegetation components at the stem elongation stage, reducing the penetration depth and thus reducing multiple interactions between vegetation components and water surface (Le Toan et al., 1989). This characteristic was also reported by Nguyen et al. (2016) and Mansaray et al. (2017). In this study, we only considered selecting the best single polarization or ratio to differentiate rice, other crops and fallow. However, since the VV channel also exhibited significant difference at the crop establishment stage between rice and others, further analysis could be done to reduce misclassification between rice and others by introducing VV information into the classifiers.

5.2.2. Temporal variations of Sentinel-1A data

The Sentinel-1A backscatter showed strong temporal variations for rice, other crops and fallow at VH polarization (Figure 4.5). These variations could be utilized to mask out non-rice areas and identify rice from the other crops and fallow on an annual basis.

The low backscatter prior to planting and high backscatter during the growth were the most striking characteristics for rice fields compared with other land-cover types. In this study, using VH-polarized signatures, we observed that the peak would occur between the stem elongation and the end of the reproductive phase, which is followed by a slight decrease at the ripening stage due to the plant drying (Le Toan et al., 1997). This is in agreement with the findings of Inoue et al. (2002) that the C-band remained sensitive to vegetation changes until late in the middle growth stage. In comparison to X-band SAR data, such as from CSK, the maximum backscatters were expected from tillering to stem elongation due to its sensitivity to early growth changes (Asilo et al., 2014). This agrees with previous studies that the temporal behaviours of backscatter for rice vary with the frequencies and polarizations.

The temporal backscatters from other crops, such as maize, onion, okra, showed little differences between them at land preparation and the growth stages, but their growth duration varied. For example, the maturity duration of okra was 45 days, remarkably shorter than those for maize (120 days), this information can be utilized to discriminate them from each other by selecting distinct SAR acquisition period in further studies. Interestingly, fallow land exhibited different temporal patterns in DS and WS. In the WS, fallow land was a mixture of water and aquatic plants, which could act as multiple scatterers, resulting in higher backscatters compared with the dry fallow land.

5.2.3. Parameter definition and temporal features extraction

This study defined the six parameters (Table 3.1) and corresponding temporal features (Table 3.2) to detect rice cropping patterns based on the field data collected during the field survey and temporal SAR signatures. These parameters were derived from an agronomic perspective, which required a priori knowledge of study area, crop calendar, maturity duration, crop practices from field survey. The SAR temporal signature is frequency and polarization dependent and also varies based on the properties of crops (Nelson et al., 2014). This implies that the parameters may need to be adapted according to the study area, crop types, crop practices, and crop calendar.

The temporal features of different cropping patterns as inputs to the classifiers were extracted from the temporal signatures within a specific timing, maximizing the unique temporal characteristics that rice fields exhibited during the flooding/planting and early growth period. The timing restricted the feature extraction window, avoiding contamination from other parts of the signature, and was estimated according to the crop planting schedules and duration between growth stages. This indicates that the timing window varies with crop calendar and growth stages.

5.2.4. Decision rules setting

A decision tree and a rule-based algorithm were used to generate the classification rules to differentiate the four rice cropping patterns (rice-rice, other-rice, rice-fallow, fallow-rice).

In this study, we have demonstrated that a rule-based classifier outperformed a decision tree classifier in terms of overall classification accuracy and kappa coefficient from the validation results. This is related to the decision strategies of the classifiers. The decision tree adopted in this study is a greedy model, meaning it makes the most optimal decision at each step, but does not take into account the global optimum (Bennett, 1994). At each step, the algorithm chooses the best result. However, choosing the best result at a given step does not ensure the optimal decision at the final leaf node of the tree. Conversely, the rule-based classifier took advantage of organic and systematic rules setting and involved the expert thinking and prior knowledge, thus yielded higher classification accuracy.

In terms of threshold selection, the decision tree could automatically generate optimal thresholds at each splitting node, while in the rule-based classifier, thresholds were selected manually and were guided by the temporal signatures. However, the samples collected from the field were limited, especially for rice-fallow and fallow-rice, which could lead to bias in the training and validation process. For a decision tree, number of samples from rice-fallow, and fallow-rice as the basis for classification were not adequate for an informed decision. We used a 10-fold cross-validation to control the tree size. This would limit the risk of overfitting but at the expense of error due to the bias in sample size. The uncertainty introduced by small samples existing in the threshold selection for the rule-based and decision tree classifiers can be mitigated with larger training samples.

5.2.5. Rice cropping patterns map

In this study, we extracted the average backscatter value of each rice field as the training and validation dataset. Consistently, the map should be created on the field level, however, due to a lack of rice field boundary information across the study site, we created the pixel-based map to give an overview of the various cropping patterns practised in the study area.

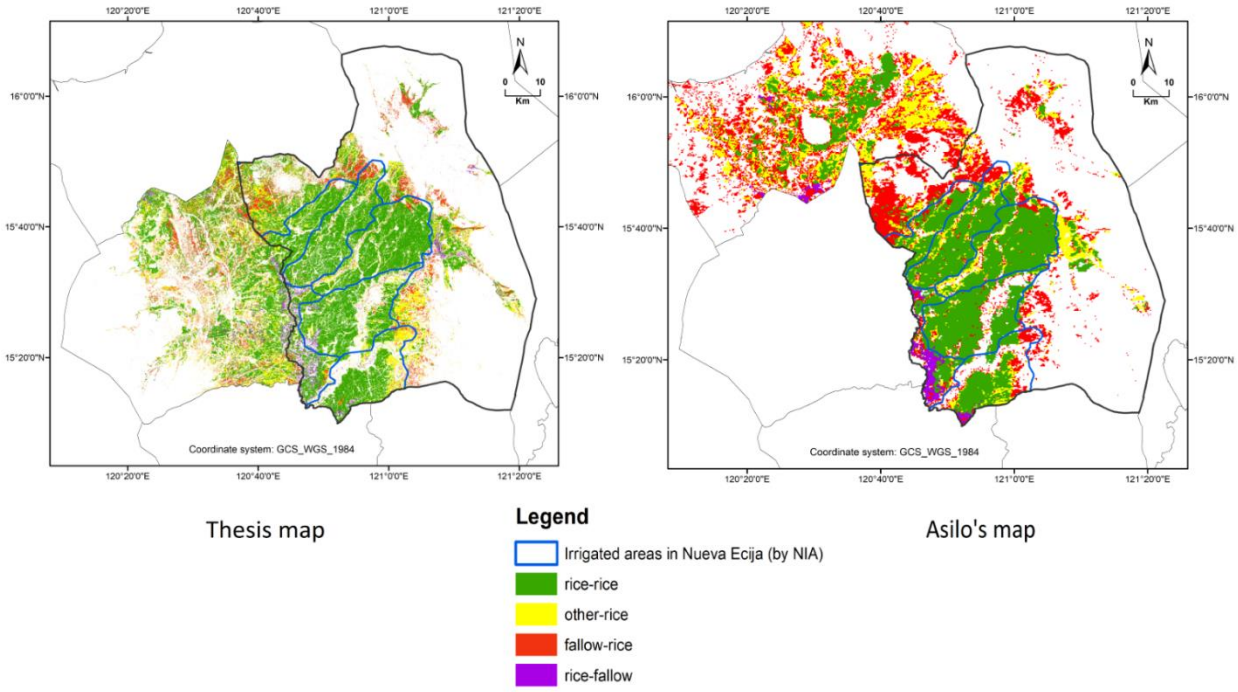

Figure 5.1 Rice cropping patterns at 2016-2017 growing seasons (obtained using rule-based classification in this thesis) **(left)** and rice cropping pattern obtained from Asilo et al. (2014) **(right)** in Nueva Ecija, the Philippines

The rule-based algorithm was then successfully applied to each pixel of the multitemporal Sentinel-1A images to mapping the rice cropping patterns in the study area. The classified map presented in Figure 5.1 shows that the rice-rice pattern was dominant and mostly located in the irrigation areas that are supported by NIA, and the fallow-rice and other-rice cropping patterns were mainly distributed at the edges of the irrigation areas. This is explained by lack of water in the DS. The rice-fallow pattern mainly existed along the big canals or rivers. Thus the rice fields were vulnerable to be flooded by the groundwater in the WS.

Asilo et al. (2014) used 250-m resolution MODIS hyper-temporal data of 5 years to derive the rice characteristics map including rice cropping patterns in Nueva Ecija and Pangasinan provinces. For the sake of comparison, we grouped the cropping patterns in the Asilo's map into rice-rice, other-rice, fallow-rice, and rice-fallow according to the NDVI class code in the initial cropping system map. As shown in Figure 5.1, the distribution of rice-rice and rice-fallow in Nueva Ecija obtained in this study has a reasonable visual agreement with the map of Asilo et al. (2014), although they have different spatial and temporal resolutions.

Although the classifier could properly detect most rice-planted areas in both seasons, some land cover types, that were not excluded by the land cover mask, caused misclassifications. In the DS, the temporal behaviour of some land covers, such as water tanks or small rivers that drained very quickly and followed by sudden vegetation growth, are similar with rice signature if the timing of the event corresponds to rice crop calendar, which leads to an increase in commission error. This type of error could be reduced using ancillary water surface mask or land cover data. Also, the temporal profile of some other crops exhibited relatively low backscatter prior to planting, and this unusual behaviour may be caused by the smoothed surface after elaborate land levelling. Discrimination of rice and other crops was challenging for such pixels. The omission errors were caused by lack of correspondence between the observed rice crop calendar and the acquisition period. In this study, some rice fields will be misclassified if the flooding/crop establishment dates exceed the SAR acquisition window, especially for early rice which is sown before November in the DS. A longer acquisition period covering the crop establishment window in the DS

could be expected to reduce such type of error. Furthermore, a lack of observations during the flooding/transplanting stage of short-duration rice fields in the WS, due to a cancellation of June 17, might casue incorrect detection of actual lowest backscatter, thus increasing the chance of misclassifying rice to fallow. The aforementioned errors occur either in DS or WS contributing to the bias in the annual rice cropping patterns map.

5.3. Limitations

In the followings, we have highlighted the limitations of the study that restrict the extent to which the findings can be generalized beyond the study conditions.

(1) Limitation of field survey: To get information on annual cropping patterns, we only performed the field observations during the wet season and gathered the farming practice dates throughout one year based on farmer interviews. The accuracy of farming practice dates in both seasons relies on the good memory of farmers; even if they are all experienced, potentially inaccurate dates could be recorded during the interviews. This would result in an inaccurate link between crop calendar and SAR acquisition in the data analysis. One way to mitigate the uncertainty is to reduce time span between events and survey (and reduce farmer recall bias) by conducting a field survey in the dry season and wet season separately.

(2) Limitation of sample size: In this study, the samples of rice-fallow and fallow-rice were limited to seven and eight respectively. The size was not as desired which could be explained by the crop practice changes, extreme events and absent farmers who practised rice-fallow or fallow-rice cropping pattern. This will lead to a bias for training the classifiers and subsequently lower the performance of the classifiers. Larger training samples are expected to produce more accurate results.

(3) Limitation of classification map: Polygons have been selected as sampling unit in this study, therefore the map should be generated and assessed on the field level, however, due to lack of rice area boundary, we produced the pixel-based map to give an overview of the distribution per rice cropping pattern. This could introduce some uncertainty when the classification is inconsistent with the sampling unit.

5.4. Implications

The study has demonstrated the feasibility of using multitemporal Sentinel-1 imagery to detect rice cropping patterns using the VH channel in rice growing areas with large variations in crop planting schedules. In the study, we defined the parameters derived from an agronomic perspective, and corresponding temporal features from SAR signatures to classify rice, other crops and fallow land in two consecutive seasons. We also compared the predictive performance of decision tree and rule-based classifiers in terms of overall accuracy and kappa values.

The two research hypotheses proposed in this study, including (1) VH polarization can be used to find the most discriminatory temporal signatures for different cropping patterns, and; (2) A rule-based classifier can give the highest accuracy compared to a decision tree classifier for classifying different rice cropping patterns have been tested and proved to be true.

SAR-based rice mapping has been well studied over the past several decades, and there is still a great deal of interest and values existing in the remote sensing community. This study can help the research community to explore the potential value of using more advanced SAR systems to map the area and distribution per cropping pattern in rice-based cropping systems. Current and forthcoming SAR systems

that offer an opportunity to deliver regular and systematic acquisitions of rice-planted areas should be employed to address the possibility of rapid and timely updates on such information with slight efforts.

Furthermore, the rule-based algorithm and decision tree classifier are both applicable for annual rice cropping pattern classification over large areas using a relatively small number of training and validation observations. Other supervised classification methods (e.g., SVM) could be potentially employed to deal with SAR-based time series data. Future research in the use of SAR data with the aid of new emerging cutting-edge technologies for rice-based cropping patterns mapping are expected.

5.5. Recommendations

From our experience in this study, we propose some recommendations in the followings that can be considered in the future work regarding SAR-based rice cropping patterns detection and classification:

(1) In the field survey, the printed questionnaires could be ruined by the unexpected rainfall, and the use of tablet devices is recommended to avoid such damage as well as errors when retyping the paper-based data into a digital format.

(2) Ancillary information such as existing land cover maps or rice area boundaries can be used to improve the classification by masking out annual non-rice areas, thus avoiding potential misclassifications from other land covers. Also, optical images acquired in suitable periods, often outside the rice-growing season, can be utilized as a complement to develop such a mask (Nelson et al., 2014).

(3) The sub-class of other-rice pattern (e.g. maize-rice or okra-rice) could be further identified to add more detailed information for rice-based cropping patterns, such as exploring the possibility of selecting distinct SAR acquisition period to seperate other crops (e.g., maize, okra) that have a significant difference in the maturity durations.

(4) Adequate SAR observations than were used here are suggested to map rice cropping patterns in the areas where large variations exist in the rice planting schedules.

(5) Multi-polarization analysis can be employed to reduce misclassification between rice and others by introducing VV information into the classifiers.

6. CONCLUSION

The study utilized farmer and field surveys and time series Sentinel-1A data with 12-day revisit time and 20 m spatial resolution to detect rice cropping patterns (rice-rice, other-rice, rice-fallow, fallow-rice) in two major rice-growing provinces of the Philippines (Nueva Ecija and Tarlac). In the study, we defined the parameters derived from an agronomic perspective, and corresponding temporal features from SAR signatures to differentiate rice, other crops and fallow land. The predictive performance of decision tree and rule-based classifiers were compared in terms of overall accuracy and kappa values. The highest overall accuracy (83%) was obtained from the validation results compared to the decision tree classifier (76%). To our knowledge, this is the first time that multitemporal Sentinel-1A imagery has been used to delineate rice cropping patterns at field level a high accuracy was obtained using a rule-based algorithm.

In the study, we used time series of co (VV) and cross (VH) polarized backscatter as well as the band ratio (VV/VH) to find the most discriminatory information for separating rice from other crops and fallow land in two consecutive seasons. We demonstrated that VH was the best single polarization to classify different cropping patterns, considering the significant difference between crops at crop establishment stage and its sensitivity to rice crop growth. Further studies could explore multi-polarizations to improve the performance of the classifiers, such as introducing VV-polarized signatures at flooding/crop establishment stage.

Furthermore, the study described temporal features from the SAR time series that correspond to agronomically relevant parameters and how these could be used to discriminate between cropping patterns. A set of thresholds for these temporal features were estimated with the caveat that these are appropriate only for C-band SAR in VH polarization with an acquisition angle between 30° and 46°. The parameters were suitably tuned using expert knowledge and in-situ surveyed data according to the study location, crop type, crop calendar and crop practices. The threshold selection could be more accurate with larger training samples in future. The final classification map showed reasonable distributions of different rice cropping patterns in Nueva Ecija compared to national irrigation areas and the map derived from hyper-temporal MODIS data in the paper of Asilo et al. (2014).

Despite some limitations, the study presented the applicability of multitemporal high-resolution Sentinel-1 images for rice-based cropping pattern detection, and provided strong implications for mapping area and distribution per rice cropping pattern using more advanced SAR systems with slight efforts. Some recommendations have been proposed and could be considered in the future studies.

LIST OF REFERENCES

Arnaoudov, V., Sibayan, E. B., & Caguioa, R. C. (2015). *Adaptation and Mitigation Initiatives in Philippine Rice c ultivation*. (G. Wilde, Ed.). Retrieved from http://www.uncclearn.org/sites/default/files/inventory/u ndp04052015.pdf

Asilo, S., de Bie, K., Skidmore, A., Nelson, A., Barbieri, M., & Maunahan, A. (2014). Complementarity of t wo rice mapping approaches: Characterizing strata mapped by hypertemporal MODIS and rice padd y identification using multitemporal SAR. *Remote Sensing*, *6*(12), 12789–12814. https://doi.org/10.339 0/rs61212789

Aweto, A. O. (2013). *Shifting cultivation and secondary succession in the tropics*. (A. O. Aweto, Ed.). Wallingford: CABI. https://doi.org/10.1079/9781780640434.0000

Benediktsson, J. A., Swain, P. H., & Ersoy, O. K. (1990). Neural network approaches versus statistical met hods in classification of multisource remote sensing data. *IEEE Transactions in Geoscience and Remote Se nsing*, *28*, 540–552. Retrieved from http://ieeexplore.ieee.org/iel1/36/2143/00572944.pdf

Bennett, K. P. (1994). Global tree optimization: A non-greedy decision tree algorithm. *Computing Science and Statistics*, *26*, 156–160. Retrieved from https://www.researchgate.net/publication/2784586

Boschetti, M., Nutini, F., Manfron, G., Brivio, P. A., & Nelson, A. (2014). Comparative Analysis of Norm alised Difference Spectral Indices Derived from MODIS for Detecting Surface Water in Flooded Ric e Cropping Systems. *PLoS ONE*, *9*(2), e88741. https://doi.org/10.1371/journal.pone.0088741

Bouvet, A., Le Toan, T., & Nguyen Lam-Dao. (2009). Monitoring of the Rice Cropping System in the Me kong Delta Using ENVISAT/ASAR Dual Polarization Data. *IEEE Transactions on Geoscience and Remo te Sensing*, *47*(2), 517–526. https://doi.org/10.1109/TGRS.2008.2007963

Breiman, L.;Friedman, J.H.;Olshen, R.A.;Stone, C. J. (1984). *Classification and Regression Trees*. *Proceedings of th e National Academy of Sciences of the United States of America*. New York: Chapman & Hall.

Climatic Research Unit of University of East Anglia. (2015). Average monthly rainfall for philippines form 1901-2015. Retrieved August 11, 2017, from http://sdwebx.worldbank.org/climateportal/index.cf m?page=country_historical_climate&ThisCCode=PHL

Cuerdo, G., Villano, L., Gutierrez, M. A., Garcia, C., Laborte, A., Boschetti, M., & Nelson, A. (2013). The when and where of rice. *Rice Today*, *12*(2), 32–33. Retrieved from https://www.scribd.com/documen t/135034694/RT-Vol-12-No-2-the-When-and-Where-of-Rice#fullscreen=1

Dalle, S. P., & Blois, S. De. (2006). Shorter Fallow Cycles Affect the Availability of Noncrop Plant Resour ces in a Shifting Cultivation System. *Ecology And Society*, *11*(2), 2. Retrieved from https://www.ecolog yandsociety.org/vol11/iss2/art2/

De Datta, S. K. (1981). *Principles and practices of rice production*. New York: Wiley.

Deschamps, B., McNairn, H., Shang, J., & Jiao, X. (2012). Towards operational radar-only crop type classi fication: comparison of a traditional decision tree with a random forest classifier. *Canadian Journal of Remote Sensing*, *38*(1), 60–68. https://doi.org/10.5589/m12-012

ESA. (2013). *Sentinel-1 user handbook*. *European Space Agency technical note*. https://doi.org/10.1017/CBO9781 107415324.004

FAO. (1996). Agro-Ecological Zoning Guidelines. *FAO Soils Bulletin 76*, 3–5. Retrieved from https://ww w.mpl.ird.fr/crea/taller-colombia/FAO/AGLL/pdfdocs/aeze.pdf

FAO. (2005). Crops and cropping systems. In *Conservation Agriculture: A manual for farmers and extension worke rs in Africa*. (pp. 104–115). International Institute of Rural Reconstruction, Nairobi; African Conserva tion Tillage Network, Harare. Retrieved from http://www.fao.org/ag/ca/africatrainingmanualcd/pd f files/06crop1.pdf

Friedl, M. A., & Brodley, C. E. (1997). Decision tree classification of land cover from remotely sensed data . *Remote Sensing of Environment*, *61*(3), 399–409. https://doi.org/10.1016/S0034-4257(97)00049-7

Gilbertson, J. K., Kemp, J., & van Niekerk, A. (2017). Effect of pan-sharpening multi-temporal Landsat 8 imagery for crop type differentiation using different classification techniques. *Computers and Electronics in Agriculture*, *134*, 151–159. https://doi.org/10.1016/j.compag.2016.12.006

Gislason, P. O., Benediktsson, J. A., & Sveinsson, J. R. (2006). Random forests for land cover classificatio n. In *Pattern Recognition Letters* (Vol. 27, pp. 294–300). https://doi.org/10.1016/j.patrec.2005.08.011

Gumma, M. K., Thenkabail, P. S., Maunahan, A., Islam, S., & Nelson, A. (2014). Mapping seasonal rice cr opland extent and area in the high cropping intensity environment of Bangladesh using MODIS 500 m data for the year 2010. *ISPRS Journal of Photogrammetry and Remote Sensing*, *91*, 98–113. https://doi.o rg/10.1016/j.isprsjprs.2014.02.007

Guo, L., Pei, Z., Ma, S., Sun, J., & Shang, J. (2014). Study of Rice Identification during Early Season Using Multi-polarization TerraSAR-X Data. In D. Li & Y. Chen (Eds.), *Computer and Computing Technologies i n Agriculture VII* (pp. 337–347). Springer, Berlin, Heidelberg. https://doi.org/10.1007/978-3-642-54 344-9_40

Hijmans, R. (2007). The where and how of rice. *Rice Today*, *6*(3), 19–21. Retrieved from https://www.scrib d.com/document/34620921/Rice-Today-Vol-6-No-3

Ikuenobe, C. E., & Anoliefo, G. O. (2003). Influence of Chromolaena odorata and Mucuna pruriens fallo w duration on weed infestation. *Weed Research*, *43*(3), 199–207. https://doi.org/10.1046/j.1365-3180. 2003.00334.x

Inoue, Y., Kurosu, T., Maeno, H., Uratsuka, S., Kozu, T., Dabrowska-Zielinska, K., & Qi, J. (2002). Seaso n-long daily measurements of multifrequency (Ka, Ku, X, C, and L) and full-polarization backscatter signatures over paddy rice field and their relationship with biological variables. *Remote Sensing of Enviro nment*, *81*(2–3), 194–204. https://doi.org/10.1016/S0034-4257(01)00343-1

Jonsson, P., & Eklundh, L. (2002). Seasonality extraction by function fitting to time-series of satellite sens or data. *IEEE Transactions on Geoscience and Remote Sensing*, *40*(8), 1824–1832. https://doi.org/10.1109 /TGRS.2002.802519

Koshy, P., Nair, M., & Kumar, T. (2008). *Pest and disease management handbook*. (A. D. V., Ed.) (1st ed.). Chic hester: John Wiley & Sons.

Kucuk, C., Taskin, G., & Erten, E. (2016). Paddy-Rice Phenology Classification Based on Machine-Learni ng Methods Using Multitemporal Co-Polar X-Band SAR Images. *IEEE Journal of Selected Topics in Ap plied Earth Observations and Remote Sensing*, *9*(6), 2509–2519. https://doi.org/10.1109/JSTARS.2016.25 47843

Laborte, A. G., de Bie, K. C. A. J. M., Smaling, E. M., Moya, P. F., Boling, A. A., & Van Ittersum, M. K. (2012). Rice yields and yield gaps in Southeast Asia: Past trends and future outlook. *European Journal of Agronomy*, *36*(1), 9–20. https://doi.org/10.1016/j.eja.2011.08.005

Lavreniuk, M., Kussul, N., Meretsky, M., Lukin, V., Abramov, S., & Rubel, O. (2017). Impact of SAR Dat a Filtering on Crop Classification Accuracy. *IEEE First Ukraine Conference on Electrical and Computer En gineering (UKRCON)*, 912–916. https://doi.org/10.1109/UKRCON.2017.8100381

Le Toan, T., Laur, H., Mougin, E., & Lopes, A. (1989). Multitemporal and dual-polarization observations of agrcultural vegetation covers by X-band SAR images. *IEEE Transactions on Geoscience and Remote Se nsing*, *27*(6), 709–718. https://doi.org/10.1109/TGRS.1989.1398243

Le Toan, T., Ribbes, F., Li-Fang Wang, Floury, N., Kung-Hau Ding, Jin Au Kong, … Kurosu, T. (1997). Rice crop mapping and monitoring using ERS-1 data based on experiment and modeling results. *IE EE Transactions on Geoscience and Remote Sensing*, *35*(1), 41–56. https://doi.org/10.1109/36.551933

Lemp, D., & Koch, B. (2009). Forest monitoring using TerraSAR-X data—evaluation of processing meth ods and first results. *Proceedings of TerraSAR-X Science Meeting*, (March 2014). Retrieved from https:// www.researchgate.net/publication/260920517

Manjunath, K. R., Kundu, N., & Panigrahy, S. (2006). Analysis of cropping pattern and crop rotation usin g multi-date, multi- sensor and multi-scale remote sensing data: case study for the state of West Beng al, India K., *6411*(2006), 64110O–64110O–6. https://doi.org/10.1117/12.693921

Mansaray, L., Huang, W., Zhang, D., Huang, J., & Li, J. (2017). Mapping Rice Fields in Urban Shanghai, S outheast China, Using Sentinel-1A and Landsat 8 Datasets. *Remote Sensing*, *9*(3), 257. https://doi.org/ 10.3390/rs9030257

Mansaray, L. R., Zhang, D., Zhou, Z., & Huang, J. (2017). Evaluating the potential of temporal Sentinel-1 A data for paddy rice discrimination at local scales. *Remote Sensing Letters*, *8*(10), 967–976. https://doi. org/10.1080/2150704X.2017.1331472

Martínez-Casasnovas, J. A., Martín-Montero, A., & Casterad, M. A. (2005). Mapping multi-year cropping p atterns in small irrigation districts from time-series analysis of Landsat TM images. *European Journal of Agronomy*, *23*(2), 159–169. https://doi.org/10.1016/j.eja.2004.11.004

McNairn, H., Champagne, C., Shang, J., Holmstrom, D., & Reichert, G. (2009). Integration of optical and Synthetic Aperture Radar (SAR) imagery for delivering operational annual crop inventories. *ISPRS Jo urnal of Photogrammetry and Remote Sensing*, *64*(5), 434–449. https://doi.org/10.1016/j.isprsjprs.2008.07. 006

McNairn, H., & Shang, J. (2016). A Review of Multitemporal Synthetic Aperture Radar (SAR) for Crop M onitoring. In Y. Ban (Ed.), *Multitemporal Remote Sensing* (pp. 317–340). Springer International Publishi ng. https://doi.org/10.1007/978-3-319-47037-5_15

Meier, E., Frei, U., & Nüesch, D. (1993). Precise terrain corrected geocoded images. In *SAR Geocoding: Dat*

a and Systems (pp. 173–185).
Moya, P., Kajisa, K., Barker, R., Mohanty, S., Gascon, F., Rose, M., & Valentin, S. (2015). *Changes in rice far ming in the Philippines: Insights from five decades of a household-level survey*. Los Baños, Philippines: Internatio nal Rice Research Institute.
Myint, S. W., Gober, P., Brazel, A., Grossman-Clarke, S., & Weng, Q. (2011). Per-pixel vs. object-based cl assification of urban land cover extraction using high spatial resolution imagery. https://doi.org/10. 1016/j.rse.2010.12.017
Nelson, A., Setiyono, T., Rala, A. B., Quicho, E. D., Raviz, J. V., Abonete, P. J., … Ninh, N. H. (2014). To wards an operational SAR-based rice monitoring system in Asia: Examples from 13 demonstration si tes across Asia in the RIICE project. *Remote Sensing*, *6*(11), 10773–10812. https://doi.org/10.3390/rs 61110773
Nguyen, D. B., Clauss, K., Cao, S., Naeimi, V., Kuenzer, C., & Wagner, W. (2015). Mapping Rice Seasonal ity in the Mekong Delta with multi-year envisat ASAR WSM Data. *Remote Sensing*, *7*(12), 15868–1589 3. https://doi.org/10.3390/rs71215808
Nguyen, D. B., Gruber, A., & Wagner, W. (2016). Mapping rice extent and cropping scheme in the Mekon g Delta using Sentinel-1A data. *Remote Sensing Letters*, *7*(12), 1209–1218. https://doi.org/10.1080/215 0704X.2016.1225172
Nguyen, D. B., & Wagner, W. (2017). European Rice Cropland Mapping with Sentinel-1 Data: The Medit erranean Region Case Study. *Water*, *9*(6), 392. https://doi.org/10.3390/w9060392
Nguyen, T. T. H., De Bie, C. A. J. M., Ali, A., Smaling, E. M. A., & Chu, T. H. (2012). Mapping the irrigat ed rice cropping patterns of the Mekong delta, Vietnam, through hyper-temporal SPOT NDVI imag e analysis. *International Journal of Remote Sensing*, *33*(2), 415–434. https://doi.org/10.1080/01431161.20 10.532826
Nielsen, D. C., & Calderon, F. J. (2011). Fallow Effects on Soil. *Publications from USDA-ARS / UNL Facult y*, *Paper 1391*, 287–300. https://doi.org/10.2136/2011.soilmanagement.c19
Oyoshi, K., Tomiyama, N., Okumura, T., Sobue, S., & Sato, J. (2016). Mapping rice-planted areas using ti me-series synthetic aperture radar data for the Asia-RiCE activity. *Paddy and Water Environment*, *14*(4), 463–472. https://doi.org/10.1007/s10333-015-0515-x
Pal, M., & Mather, P. M. (2003). An assessment of the effectiveness of decision tree methods for land cov er classification. *Remote Sensing of Environment*, *86*(4), 554–565. https://doi.org/10.1016/S0034-4257(0 3)00132-9
Pandey, S., Byerlee, D., & Dawe, D. (2010). *Rice in the Global Economy: Strategic Research and Policy Issues for Fo od Security. … and Policy Issues …*. International Rice Research Institute. Retrieved from http://irri.org /resources/publications/books/rice-in-the-global-economy-strategic-research-and-policy-issues-for-food-security
Panigrahy, S., & Sharma, S. A. (1997). Mapping of crop rotation using multidate Indian Remote Sensing Sa tellite digital data. *ISPRS Journal of Photogrammetry & Remote Sensing*, *52*, 85–91. https://doi.org/10.101 6/S0924-2716(97)83003-1
Parihar, S. S., Pandey, D., Shukla, R. K., Verma, V. K., Chaure, N. K., Choudhary, K. K., & Pandya, K. S. (1999). Energetics, yield, water use and economics of rice-based cropping system. *Indian Journal of Ag ronomy*, *44*(2), 205–209. Retrieved from https://www.researchgate.net/publication/289861472
Philippine Statistics Authority. (2004). A Review of the Agriculture Sector in Central Luzon. Retrieved Au gust 6, 2017, from https://psa.gov.ph/content/review-agriculture-sector-central-luzon
Philippine Statistics Authority. (2016). Palay and Corn: Area Harvested by Cereal Type. Retrieved August 13, 2017, from http://countrystat.psa.gov.ph/?cont=10&pageid=1&ma=O80LUAHC
Potin, P., Bargellini, P., Laur, H., Rosich, B., & Schmuck, S. (2012). Sentinel-1 mission operations concept. In *2014 IEEE International Geoscience and Remote Sensing Symposium* (pp. 1745–1748). Quebec City, QC, Canada: IEEE. https://doi.org/10.1109/IGARSS.2012.6351183
Randriamalala, J. R., Hervé, D., Randriamboavonjy, J.-C., & Carrière, S. M. (2012). Effects of tillage regim e, cropping duration and fallow age on diversity and structure of secondary vegetation in Madagascar . *Agriculture, Ecosystems & Environment*, *155*, 182–193. https://doi.org/10.1016/j.agee.2012.03.020
Ripley, B. D. (1996). *Pattern recognition and neural networks*. Cambridge University Press.
Rosenthal, W., Blanchard, B., & Blanchard, A. (1985). Visible/Infrared/Microwave Agriculture Classificati on, Biomass, and Plant Height Algorithms. *IEEE Transactions on Geoscience and Remote Sensing*, *GE-23*(2), 84–90. https://doi.org/10.1109/TGRS.1985.289404
Sakamoto, T. (2009). *Spatio-temporal Analysis of Agriculture in the Vietnamese Mekong Delta using MODIS Imagery . Bulletin of the National Institute of Agro-Environmental Sciences*. National Institute for Agro–Environment

al Science. Retrieved from http://www.naro.affrc.go.jp/archive/niaes/sinfo/publish/bulletin/niaes26-1.pdf
Salehi, B., Daneshfar, B., & Davidson, A. M. (2017). Accurate crop-type classification using multi-tempora l optical and multi-polarization SAR data in an object-based image analysis framework. *International Jo urnal of Remote Sensing*, *38*(14), 4130–4155. https://doi.org/10.1080/01431161.2017.1317933
Salehi, B., Zhang, Y., & Zhong, M. (2013). A Combined Object- and Pixel-Based Image Analysis Framew ork for Urban Land Cover Classification of VHR Imagery. *Photogrammetric Engineering & Remote Sensin g*, *79*(11), 999–1014. https://doi.org/10.14358/PERS.79.11.999
Shao, Y., Fan, X., Liu, H., Xiao, J., Ross, S., Brisco, B., … Staples, G. (2001). Rice monitoring and product ion estimation using multitemporal RADARSAT. *Remote Sensing of Environment*, *76*(3), 310–325. https: //doi.org/10.1016/S0034-4257(00)00212-1
Singh, M. K., Singh, P., & Chitale, S. (2014). *Intercropping under rice-based cropping system : an experimental study o n productivity and profitability* (1st ed.). Hamburg: Diplomica Verlag.
Son, N.-T., Chen, C.-F., Chen, C.-R., Duc, H.-N., & Chang, L.-Y. (2013). A Phenology-Based Classificatio n of Time-Series MODIS Data for Rice Crop Monitoring in Mekong Delta, Vietnam. *Remote Sensing*, *6*(1), 135–156. https://doi.org/10.3390/rs6010135
Soo Chin Liew, Suan-Pheng Kam, To-Phuc Tuong, Ping Chen, Vo Quang Minh, & Hock Lim. (1998). Ap plication of multitemporal ERS-2 synthetic aperture radar in delineating rice cropping systems in the Mekong River Delta, Vietnam. *IEEE Transactions on Geoscience and Remote Sensing*, *36*(5), 1412–1420. ht tps://doi.org/10.1109/36.718845
Staver, C. (1991). The Role of Weeds in the Productivity of Amazonian Bush Fallow Agriculture. *Experime ntal Agriculture*, *27*(3), 287. https://doi.org/10.1017/S0014479700019013
Steinmann, H.-H., & Dobers, E. S. (2013). Spatio-temporal analysis of crop rotations and crop sequence p atterns in Northern Germany: potential implications on plant health and crop protection. *Journal of Pl ant Diseases and Protection*, *120*(2), 85–94. https://doi.org/10.1007/BF03356458
Stewart, R. E. (1999). Aricultural technology. In *Encyclopædia Britannica*. Encyclopædia Britannica, inc. Retri eved from https://www.britannica.com/technology/agricultural-technology
Swain, P. H., & Hauska, H. (1977). The decision tree classifier: Design and potential. *IEEE Transactions on Geoscience Electronics*, *15*(3), 142–147. https://doi.org/10.1109/TGE.1977.6498972
Umaerus, V. (1992). Crop rotation in relation to crop protection. *Netherlands Journal of Plant Pathology*, *98*(S2), 241–249. https://doi.org/10.1007/BF01974491
Vergara, B. S. (1992). *A farmer's primer on growing rice*. *Field Crops Research* (Vol. 4). lnternational Rice Researc h Institute. https://doi.org/10.1016/0378-4290(81)90059-9
Waheed, T., Bonnell, R. B., Prasher, S. O., & Paulet, E. (2006). Measuring performance in precision agricu lture: CART-A decision tree approach. *Agricultural Water Management*, *84*(1–2), 173–185. https://doi.o rg/10.1016/j.agwat.2005.12.003
Winch, T. (2006). Section 1 The principles and practices used in agriculture and horticulture. In *Growing Fo od* (pp. 1–103). Dordrecht: Springer Netherlands. https://doi.org/10.1007/978-1-4020-4975-0_1
Xiao, X., Boles, S., Frolking, S., Li, C., Babu, J. Y., Salas, W., & Moore, B. (2006). Mapping paddy rice agri culture in South and Southeast Asia using multi-temporal MODIS images. *Remote Sensing of Environme nt*, *100*(1), 95–113. https://doi.org/10.1016/j.rse.2005.10.004
Zheng, B., Myint, S. W., Thenkabail, P. S., & Aggarwal, R. M. (2015). A support vector machine to identif y irrigated crop types using time-series Landsat NDVI data. *International Journal of Applied Earth Observ ations and Geoinformation*, *34*, 103–112. https://doi.org/10.1016/j.jag.2014.07.002

7. APPENDICES

Appendix I Questionaire and plot sheet

A. Farmer interview sheet [one sheet per plot, maximum of three plots per farmer]

0	HHID				
1	What is the size of the plot (ha)	____ha			
2	How many crops did you grown between Nov 2016 and now?	____crops			
	Questions (ask them crop by crop)	1st crop	2nd crop	3rd crop	Notes/codes
3	What crop				Can be R(ice), M(aize), (O)nion, B(ean) or F(allow) etc.
4	Water source for this crop If irrigated, when did irrigation start? If rainfed, when did rainfall start?				IR or RF Month and week (1, 2, 3, 4) Month and week (1, 2, 3, 4)
5	At the start of the season, was there too much, too little or sufficient water?				Too much water [TM], too little water [TL], sufficient [S].
6	Was part of the plot used as a seed bed for this crop (rice only)?				
7	What was the crop establishment method (rice only)				TP, DDS, WDS
8	What was the age of seedlings (transplanted rice only)				Number of days old
9	What was the method of crop establishment				Manual or mechanical
10	Date of land preparation (clearing)				Month and week (1, 2, 3, 4)
11	Date of flooding (rice only)				Month and week (1, 2, 3, 4)
12	Date of establishment of crop				Month and week (1, 2, 3, 4)
13	Date of flowering				Month and week (1, 2, 3, 4)
14	Date of harvest (current crop can be expected harvest date)				Month and week (1, 2, 3, 4)
15	What was the method of harvesting				Manual or mechanical
16	Did you ratoon the rice (rice only)				Yes or no
17	What was the yield including those paid for rent and taken away as payment for harvesting (current crop can be expected yield)				Make a note if this is in cavans and ask how many kg per cavan, this varies by farmer (Cavan: mass unit → ± 50 kg) Also note the unit for the yield of other crops.
18	Notes:				

B. Plot data sheet [one sheet per plot, maximum of three plots per farmer]

0	HHID		
1	Date and time		
2	Measurements	S/V/K	
3	Plot No.		
4	Corner Coordinates	X1: X2: X3: X4:	Y1: Y2: Y3: Y4:
5	Field length and width (m)	L:	W:
6	Field size (ha)	field measurement: ha	
7	Soil condition	Dry/Wet/Flooding with …. cm water level	
8	Plant height (cm), 3 reps	(a) (b) (c) (d) average: cm	
9	Rice plant age	days	
10	Sketch *If part of the field was used as a seed bed, mark the approximate location. Take photos of the field and the surrounding area (N,E,S and W). Draw sketch facing to the north*		
11	Notes:		

Appendix II Selected farmers in each village

No	Municipality	Village	HHID	Lat	Long
1	**Bongabon**	Macabaclay	8181	15.637154	121.173828
2			8185	15.637883	121.17387
3			8188	15.639088	121.175738
4			8189	15.640583	121.178065
5			8198	15.639113	121.174824
6			8199	15.63766	121.174089
7			8200	15.636871	121.172034
8		Pesa	8201	15.647196	121.185776
9			8202	15.647014	121.185785
10			8204	15.647792	121.184303
11			8205	15.647363	121.184589
12			8206	15.647183	121.186081
13			8214	15.648665	121.185147
14			8215	15.648314	121.186161
15			8218	15.647307	121.184457
16			8220	15.64686	121.186174
17			8223	15.655901	121.136342
18		Vega	8225	15.654647	121.135292
19			8229	15.656804	121.135743
20			8231	15.651409	121.139313
21			8232	15.650769	121.138887
22			8233	15.651577	121.139635
23			8234	15.651452	121.139421
24			8235	15.654723	121.134617
25			8237	15.655658	121.137166
26			8238	15.656644	121.135721
27			8239	15.655319	121.136891
28			8240	15.655512	121.13773
29			8224	15.655104	121.134856
30		Calaanan	8161	15.65933	121.22579
31			8162	15.65934	121.22703
32			8165	15.66004	121.22923
33			8178	15.65924	121.2273
34			8179	15.65747	121.23242
35			8180	15.65941	121.226
36	**Talugtug**	Villa Rosario	9001	15.772023	120.845691
37			9002	15.767346	120.841478
38			9003	15.771166	120.844586
39			9004	15.772027	120.845804
40			9005	15.775102	120.846228
41			9006	15.774137	120.846268

42			9007	15.767838	120.841808
43			9008	15.771375	120.8447
44			9010	15.772779	120.845741
45			9011	15.769873	120.844174
46			9012	15.770057	120.84437
47			9013	15.772254	120.845262
48			9016	15.770292	120.843596
49			9017	15.77109	120.844517
50			9018	15.774233	120.846229
51			9019	15.77205	120.845138
52			9020	15.771305	120.844242
53			9021	15.783211	120.833315
54		Alula	9022	15.782398	120.832111
55			9023	15.782631	120.83228
56			9024	15.784167	120.833196
57			9027	15.784553	120.835266
58			9030	15.784986	120.83285
59			9034	15.786046	120.835197
60			9035	15.785904	120.836127
61		Cabiangan	8961	15.775656	120.808075
62			8962	15.775242	120.808698
63			8963	15.774803	120.807665
64			8964	15.775265	120.807808
65			8965	15.775738	120.809053
66			8972	15.774819	120.807462
67			8976	15.774341	120.808444
68			8977	15.774425	120.80822
69			8978	15.774956	120.807228
70	**Tarlac city**	Villa Bacolor	9621	15.50579	120.68142
71			9623	15.5095	120.67991
72			9624	15.50544	120.68113
73			9627	15.51066	120.68023
74			9632	15.50894	120.67947
75			9634	15.50555	120.68094
76			9635	15.5095	120.67989
77			9636	15.51034	120.68045
78			9661	15.490537	120.6668
79		San Manuel	9664	15.490939	120.668802
80			9665	15.490517	120.668457
81			9666	15.489607	120.6707
82			9673	15.49244002	120.666911
83			9674	15.491444	120.668231
84			9676	15.491	120.668603
85	**La Paz**	Macalong	9466	15.465353	120.722513

86			9468	15.46359	120.723822
87			9469	15.464299	120.721654
88			9470	15.465287	120.721958
89			9471	15.466062	120.721477
90			9472	15.46438	120.720994
91			9474	15.465537	120.721336
92			9482	15.428895	120.728493
93		Rizal	9483	15.43091	120.726111
94			9484	15.431621	120.726519
95			9486	15.429969	120.725953
96			9487	15.430603	120.727047
97			9491	15.430366	120.725631
98			9492	15.430254	120.725986
99			9496	15.430658	120.726204
100	**Santa Rosa**	Berang	8803	15.418197	120.909326
101			8805	15.415517	120.920809
102			8806	15.415713	120.920438
103			8808	15.416099	120.920387
104			8809	15.415442	120.921249
105			8820	15.449729	120.984605
106		San Isridro	8850	15.42614	120.892789
107			8851	15.428624	120.892477
108			8856	15.42708398	120.891795
109			8858	15.428954	120.892275
110			8859	15.428974	120.893172
111			8860	15.428777	120.892678
112			8855	15.425416	120.893178
113	**Aliaga**	Pantoc	8121	15.525776	120.847869
114			8124	15.52507	120.847408
115			8127	15.523078	120.845842
116			8128	15.522411	120.845784
117			8130	15.522748	120.845818
118			8131	15.514855	120.84769
119			8135	15.52747	120.847479
120			8136	15.528003	120.847308
121			8138	15.512664	120.849657
122			8139	15.516001	120.84799
123			8140	15.520488	120.848614
124		San Felipe (Old)	8101	15.50143	120.908941
125			8102	15.499338	120.908059
126			8104	15.50173	120.909003
127			8105	15.499482	120.907017
128			8108	15.501296	120.907181
129			8110	15.499691	120.908244

130			8111	15.50031	120.908354
131			8115	15.499929	120.907045
132			8116	15.501894	120.907604
133			8118	15.501567	120.905941

Appendix III Scheduled fieldwork plan

Day		Villages visited by Vidya, Sravan & Kuan	
1	Wednesday	Aliaga (Pantoc)	Tarlac city (Villa Bacolor)
2	Thursday	Aliaga (San Felipe)	Tarlac city (San Manuel)
3	Friday	Santa Rosa (Berang)	Lapaz (Macalong)
4	Saturday	Santa Rosa (San Isidro)	Lapaz (Rizal)
5	Sunday	Break	
6	Monday	Bongabon (Macabaklay and Pesa)	
7	Tuesday	Bongabon (Calaanan)	
8	Wednesday	Bongabon (Vega)	
9	Thursday	Talugtug (Alula)	
10	Friday	Talugtug (Villa Rosario)	
11	Saturday	Talugtug (Cabiangan)	

Appendix IV P-values of ANOVA tests between Onion (12), Maize (7) and Okra (5) at LP, CE, and HA

Polarization or band ratio	Farming operation	P-value
VH	LP	0.7677
	CE	0.3160
	HA	0.0597
VV	LP	0.6634
	CE	0.3578
	HA	0.0043**
VV/VH	LP	0.6774
	CE	0.2838
	HA	0.6133

(* statistically significant at 0.05 level; ** statistically significant at 0.01 level; *** statistically significant at 0.001 level)

Appendix V Temporal features for training and validation plots

A. Temporal features for training plots

Plot ID	Cropping pattern	Temporal features					
		DS					WS
		a	*b*	*c*	*d*	*e*	*f*
9634	rice-rice	-20.1687	-14.7444	5.424295	-13.794	12	-16.2834
9636	rice-rice	-18.8323	-14.392	4.440281	-13.7781	72	-15.5773

9621	rice-rice	-18.1729	-15.0531	3.119817	-15.0894	60	-15.7706
9632	rice-rice	-16.078	-14.6851	1.392883	-14.931	48	-14.5371
9623	rice-rice	-19.511	-14.7944	4.716621	-13.8128	84	-15.2728
9673	rice-rice	-17.9984	-14.7479	3.250472	-14.2863	48	-14.546
9661	rice-rice	-21.9772	-15.2303	6.746912	-16.0964	60	-15.7822
9664	rice-rice	-21.6528	-15.8702	5.782611	-15.3972	12	-16.6889
9674	rice-rice	-18.8295	-14.0961	4.733413	-15.932	48	-15.5343
9666A	rice-rice	-21.7814	-16.166	5.615371	-13.2488	72	-16.9726
8206A	rice-rice	-19.4532	-15.4812	3.972027	-16.9181	24	-15.2536
9030	rice-rice	-19.5626	-14.603	4.959586	-16.7516	12	-15.7212
9023	rice-rice	-15.8728	-14.5717	1.30107	-17.1178	24	-24.5559
9035	rice-rice	-17.1318	-14.9188	2.212987	-18.0544	48	-15.5552
9496	rice-rice	-19.76	-14.0859	5.674139	-14.8218	72	-16.486
9491	rice-rice	-18.9834	-14.5964	4.386983	-13.3194	72	-16.3945
9483	rice-rice	-18.9556	-16.043	2.912678	-15.1685	72	-16.7626
9492A	rice-rice	-19.3042	-16.1486	3.15564	-14.3129	84	-16.5034
9486	rice-rice	-19.6795	-14.925	4.754493	-16.0887	60	-16.0297
9470	rice-rice	-20.832	-15.4952	5.336856	-12.7317	60	-16.4647
9474A	rice-rice	-21.3842	-15.598	5.78622	-18.3143	12	-14.7001
9468B	rice-rice	-19.1338	-14.6162	4.517618	-15.7302	12	-14.9754
9003B	rice-rice	-18.9459	-14.7558	4.19012	-17.8892	84	-14.5559
9019	rice-rice	-18.6871	-13.3308	5.35627	-17.0877	60	-15.1479
9011	rice-rice	-18.8499	-15.9999	2.849981	-19.049	60	-16.1508
9020	rice-rice	-18.1046	-14.9899	3.114747	-18.3229	84	-15.8864
9007	rice-rice	-19.2213	-15.3782	3.843146	-17.8921	84	-15.9624
9012	rice-rice	-19.5363	-16.3892	3.147133	-18.5359	84	-15.6255
9002	rice-rice	-21.9674	-13.7911	8.176311	-16.7394	84	-16.9036
8962B	rice-rice	-19.4335	-14.7293	4.704169	-15.8058	84	-15.9446
8963	rice-rice	-21.467	-15.6262	5.840783	-15.5233	84	-17.1345
8977	rice-rice	-19.83	-14.7534	5.076607	-15.6859	72	-15.434
8965	rice-rice	-19.7766	-15.1393	4.637328	-15.7652	84	-16.0628
8974	rice-rice	-20.4781	-14.9848	5.49331	-17.2913	12	-16.2644
8976	rice-rice	-18.9536	-15.4082	3.545425	-15.5968	84	-15.1943
8198	rice-rice	-19.7508	-15.0714	4.679321	-14.094	60	-16.1645
8200	rice-rice	-22.7587	-17.0877	5.671012	-14.8809	48	-15.7068
8199A	rice-rice	-18.1779	-15.5447	2.633188	-16.2584	84	-15.9519
8188	rice-rice	-19.5183	-15.552	3.96625	-15.4384	84	-15.9222
8189	rice-rice	-20.5741	-15.4216	5.152477	-14.3948	84	-16.0803
8185A	rice-rice	-20.5714	-16.6768	3.894534	-15.4961	84	-16.9098
8185C	rice-rice	-15.91	-14.5979	1.31207	-15.7495	72	-15.815
8135	rice-rice	-20.3751	-16.2069	4.16814	-15.8086	84	-16.0017
8140A	rice-rice	-19.2142	-15.7636	3.450521	-15.2216	84	-15.8942
8140B	rice-rice	-19.2476	-12.8648	6.38285	-15.8817	84	-15.8642
8138	rice-rice	-21.5113	-16.5626	4.948712	-15.5132	84	-16.0434
9624A	other-rice	-18.6397	-13.607	5.032661	-16.9506	12	-15.9108

9627	other-rice	-20.3731	-14.8057	5.567361	-14.1014	84	-16.4963
9635	other-rice	-17.9632	-15.6578	2.305395	-15.7808	72	-16.6379
8215	other-rice	-16.9791	-14.6066	2.372521	-15.6436	36	-13.5561
8201A	other-rice	-17.3215	-13.3585	3.962976	-14.8965	60	-15.8687
8202	other-rice	-16.6131	-12.8044	3.808708	-15.6288	48	-15.9851
8201B	other-rice	-18.1718	-13.7797	4.392067	-14.95	24	-15.9416
8204	other-rice	-20.746	-14.4368	6.309162	-14.4456	84	-15.9475
8205	other-rice	-15.9342	-14.5152	1.419056	-16.3394	12	-14.9951
8178	other-rice	-15.7939	-14.1201	1.673717	-16.0561	12	-15.3683
8179	other-rice	-16.2347	-13.3823	2.852442	-14.9529	72	-15.3633
C4	other-rice	-15.5742	-13.4388	2.135335	-15.2216	36	-15.2234
C5	other-rice	-16.5959	-13.6481	2.947837	-16.2334	48	-15.4267
C6	other-rice	-15.8	-13.6739	2.126047	-14.8058	84	-15.0369
9492B	other-rice	-17.9816	-17.3382	0.643402	-15.3552	36	-16.4893
8181	other-rice	-18.692	-14.7173	3.974641	-17.2123	60	-13.8375
9471A	rice-fallow	-20.2904	-16.0987	4.191693	-14.3774	48	-13.8228
9471B	rice-fallow	-18.982	-15.7177	3.2643	-14.897	48	-13.271
9469	rice-fallow	-19.1263	-14.5855	4.540823	-16.0365	60	-13.3279
9466	rice-fallow	-19.5143	-15.552	3.962311	-16.3654	60	-12.9717
9027	fallow-rice	-17.9042	-16.0787	1.825501	-18.6339	12	-15.8958
9024B	fallow-rice	-17.4271	-15.7279	1.699221	-18.3778	36	-15.7624
9003A	fallow-rice	-19.5549	-15.6737	3.881203	-20.038	24	-16.0738
9004	fallow-rice	-17.7573	-14.4549	3.302357	-16.4951	12	-14.9184
9008	fallow-rice	-19.8074	-17.2269	2.580513	-19.7922	12	-16.3517

B. Temporal features for validation plots

HHID	Cropping pattern	*a*	*b*	*c*	*d*	*e*	*f*
8806B	rice-rice	-22.063	-14.6999	7.363094	-15.4464	72	-17.4384
8806A	rice-rice	-24.4345	-13.8312	10.60331	-14.1655	84	-17.5539
8808	rice-rice	-23.7729	-14.2697	9.503248	-14.855	84	-16.2933
8803	rice-rice	-21.7734	-14.4157	7.357779	-16.1595	84	-16.0762
8809	rice-rice	-21.9623	-14.0076	7.954718	-15.6397	84	-16.5102
8805	rice-rice	-22.6485	-14.0924	8.556197	-15.9443	84	-16.5624
8820	rice-rice	-22.0326	-14.3056	7.727028	-14.2675	72	-16.8279
8108	rice-rice	-22.0007	-14.6894	7.3113	-17.2864	84	-16.1133
8115	rice-rice	-21.461	-13.5395	7.921505	-17.2085	84	-17.0233
8118	rice-rice	-22.1463	-14.4249	7.721466	-16.9094	72	-17.6738
8110	rice-rice	-21.0954	-14.2791	6.816304	-18.1604	84	-16.7061
8102	rice-rice	-22.1748	-14.8698	7.305009	-17.9835	60	-16.0471
8860	rice-rice	-22.8656	-13.843	9.022594	-16.3999	84	-16.3473
8856	rice-rice	-22.7857	-13.4628	9.322948	-15.6097	84	-16.5502
8850A	rice-rice	-20.0763	-14.8925	5.183803	-15.5967	84	-15.6747
8859A	rice-rice	-18.431	-14.345	4.086022	-15.2579	84	-15.4618
8859B	rice-rice	-21.3135	-14.0647	7.248782	-18.1783	84	-16.0745
8855A	rice-rice	-22.7408	-14.8356	7.905171	-16.2912	84	-16.3744

8855B	rice-rice	-23.2863	-14.6741	8.612189	-17.8055	60	-16.5925
SI6A	rice-rice	-21.8115	-14.9664	6.845038	-14.8172	72	-17.3693
SI6B	rice-rice	-22.5108	-12.8923	9.618497	-16.2608	84	-17.0368
8224	rice-rice	-21.4137	-17.9072	3.506465	-14.9676	84	-15.8316
P8	rice-rice	-20.1466	-15.5287	4.61787	-14.7457	84	-16.1855
P7A	rice-rice	-22.3913	-15.6336	6.757657	-13.1402	84	-15.3415
8225	rice-rice	-19.7991	-14.5291	5.270024	-16.4162	84	-15.3505
8235	rice-rice	-21.696	-15.5092	6.186802	-16.8466	72	-16.5618
8240	rice-rice	-22.738	-16.5281	6.209906	-16.2223	84	-18.1113
8238A	rice-rice	-16.9852	-13.7341	3.251104	-15.3197	84	-15.965
8232A	rice-rice	-22.0958	-16.8022	5.293559	-14.9611	84	-16.7886
9024A	rice-rice	-17.0048	-14.0577	2.94713	-18.3252	12	-15.0014
8962A	rice-rice	-19.5389	-15.0683	4.470621	-15.7933	84	-16.0044
8185B	other-rice	-16.8648	-13.5183	3.346462	-14.8023	12	-15.2746
8136	other-rice	-17.872	-13.0894	4.782585	-13.8692	48	-14.7107
8124	other-rice	-20.1865	-14.6567	5.529741	-13.5411	84	-16.2892
8121	other-rice	-17.5195	-13.2335	4.285998	-14.2612	48	-15.2316
8140C	other-rice	-16.7809	-12.8666	3.91429	-13.4635	12	-15.9755
8237	other-rice	-18.4196	-15.2927	3.126928	-14.55	48	-15.4528
8234	other-rice	-20.8001	-13.8268	6.973326	-14.9518	72	-16.9726
8238B	other-rice	-19.334	-16.9436	2.390334	-14.6592	60	-15.947
9666B	other-rice	-21.4653	-13.502	7.963343	-14.4154	72	-16.4855
P7B	other-rice	-21.1442	-16.4407	4.703522	-14.0921	72	-15.4949
8232B	other-rice	-19.6306	-14.4783	5.152354	-14.2807	60	-16.1192
9474C	rice-fallow	-18.7286	-14.633	4.095588	-15.3611	60	-12.8466
9468A	rice-fallow	-21.3535	-15.0134	6.340054	-15.2228	48	-13.0375
9474B	rice-fallow	-20.0922	-15.7678	4.324445	-15.3789	72	-13.7162
9001	fallow-rice	-17.908	-14.7023	3.205639	-18.9371	12	-16.2932
8199B	fallow-rice	-19.1476	-15.4852	3.662388	-17.9219	60	-15.7211
8206B	fallow-rice	-19.3168	-14.8567	4.460101	-15.8441	48	-14.4366